Journal of Materials Chemistry C

ROYAL SOCIETY OF CHEMISTRY

REVIEW

View Article Online
View Journal | View Issue

Cite this: J. Mater. Chem. C, 2022, 10, 2411

Polycyclic aromatic hydrocarbon-based organic semiconductors: ring-closing synthesis and optoelectronic properties†

Qingbin Li,[ab] Yihan Zhang,[ab] Ziyi Xie,[ab] Yonggang Zhen,[c] Wenping Hu[d] and Huanli Dong *[ab]

Received 11th October 2021,
Accepted 25th November 2021

DOI: 10.1039/d1tc04866j

rsc.li/materials-c

Polycyclic aromatic hydrocarbons (PAHs) as a typical class of organic semiconductors demonstrate unique optical, electrical, magnetic and other interesting properties due to their extended conjugation and diverse structures. Ring-closing reactions are very significant for the synthesis of PAHs with various structures and optoelectronic properties, which endow them great potential for applications in organic electronics. The aim of this article is to present a concise summary on the recent advances on the ring-closing reactions for the synthesis of organic semiconductors, with a discussion on their applicable conditions, followed by their attractive applications in organic field-effect transistors (especially chiral transistors and biradicaloid-based transistors), organic solar cells, *etc.* Finally, a short conclusion and perspective are given on the further development of new ring-closing reactions toward novel PAH materials with promising applications.

[a] *Beijing National Laboratory for Molecular Sciences, Key Laboratory of Organic Solids, Institute of Chemistry, Chinese Academy of Sciences, Beijing 100190, China. E-mail: dhl522@iccas.ac.cn*
[b] *University of Chinese Academy of Sciences, Beijing 100049, China*
[c] *Beijing Advanced Innovation Center for Soft Matter Science and Engineering, State Key Laboratory of Organic–Inorganic Composites, Beijing University of Chemical Technology, Beijing 100029, China*
[d] *Tianjin Key Laboratory of Molecular Optoelectronic Sciences, Department of Chemistry, School of Science, Tianjin University and Collaborative Innovation Center of Chemical Science and Engineering, Tianjin 300072, China*

† Dedicated to Prof. Daoben Zhu on the occasion of his 80th birthday.

1. Introduction

Organic semiconductors have attracted much attention over the past several decades due to their unique optical, electrical, magnetic and other physical and chemical properties, which endow them with wide applications in many emerging fields.[1,2] For instance, under the joint effort of chemists and device scientists, organic semiconductors have been successfully applied in the field of organic field-effect transistors (OFETs),[3] organic light-emitting diodes (OLEDs),[4] and photovoltaic cells.[5] However,

Qingbin Li

Qingbin Li grew up in Gansu Province, China. He got his Bachelor's Degree from Beijing Institute of Technology in 2019. Since 2019, he has been undertaking successive postgraduate and doctoral programs of study to obtain his PhD at the Key Laboratory of Organic Solids, Institute of Chemistry, Chinese Academy of Science, Beijing, under the supervision of Prof. Huanli Dong. His research work focuses on the design and synthesis of organic optoelectronic functional materials based on polycyclic aromatic hydrocarbon systems.

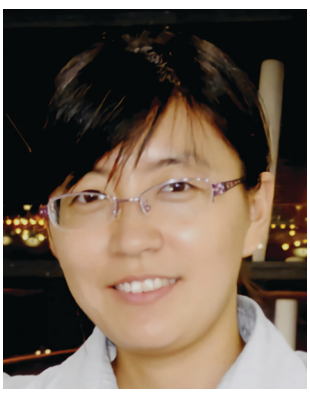

Huanli Dong

Huanli Dong is a Professor of the Institute of Chemistry, Chinese Academy of Sciences. She received her PhD Degree from this Institute in 2009 after she obtained her MS Degree from the Fujian Institute of Research on the Structure of Materials, CAS, in 2006. Her current research is focused on organic/polymeric optoelectronic materials and their device applications including organic field-effect transistors, organic light-emitting transistors, photodetectors and their circuits.

due to the high requirements of these applications, a series of material systems with excellent performances, which generally consists of a considerable number of aromatic rings and related fused structures, has been developed.[6–8] Especially, polycyclic aromatic hydrocarbons (PAHs) have become molecular libraries of organic semiconductor materials and popular material systems due to their inherent conjugated structure and strong intermolecular interaction, which result in favorable solid stacking. As a representative molecule, pentacene delivered a hole mobility of over 5 cm^2 V^{-1} s^{-1} due to its extended π-conjugated structure with ideal molecular packing.[9] With thiophene rings replacing the benzene rings, pentathienoacene as another typical PAH molecule exhibits excellent chemical stability due to its appropriate energy levels.[10] To date, various PAHs with complex structures such as chiral helicenes, biradical graphene nanosheets and spatial-structure rylene, have been developed with fascinating optical, electrical and magnetic properties and proven to be an integral part of organic semiconductors for device applications. The fast development of PAHs and their applications are largely due to the gradual maturity of their design and synthesis methodology.

In 1910, Scholl discovered the formation of an intramolecular six-membered ring when certain aromatic compounds were heated with $AlCl_3$.[11] Subsequently, this reaction had aroused widespread interest and numerous examples of π-expanded aromatic compounds were synthesized.[12,13] As molecules become more complex, especially the continuous expansion of fused ring systems, many synthetic methods have been established and developed. Reviewing the processes, ranging from simple linear acenes and planar acenes to spatial acenes and graphene nanoribbons, highlight the importance of the molecular design and synthetic approach. Focusing on the change in PAH materials synthesized *via* these methods does not only lead to highly extended conjugated structures for much higher optoelectronic performances but also may result in more interesting properties such as chirality and biradical character due to the unique features in the ring structure. These specific properties further trigger promising applications in various devices.

The aim of this article is to give special summary on the synthesis of PAH-based semiconductors and their photoelectronic properties and device applications. There is no related review regarding this topic though some reviews of ring-closing reactions have been given from a chemical point of view.[12,14–16] This article is divided into the following parts: (1) summarizing and discussing the current ring-closing reactions used in the synthesis of PAH-based organic semiconductors including Scholl-type reaction, iodine-promoted photocyclization reaction and palladium-catalyzed annulation reaction (Fig. 1); (2) current advances in the development of novel PAHs based on the above-mentioned catalyzed annulation reaction; and (3) representative promising applications of PAH-based organic semiconductors synthesized through ring-closing reactions. Finally, a brief conclusion and perspective are presented on the further development of PAHs and their related interesting research directions.

2. Ring-closing reactions and their application in the synthesis of organic semiconductors

2.1. The representative ring-closing reactions

Scholl-type reaction. The Scholl reaction is a classical dehydrogenation coupling reaction in which two molecular aryl groups are coupled in the presence of a Lewis acid.[12] As early as 1910, Scholl and coworkers discovered an intramolecular variant and employed neat anhydrous $AlCl_3$ at 140 °C for 45 min.[11] The significance of the "Scholl reaction" is that a new hexagonal all-sp^2-carbon ring is formed with high atom-efficiency. After the discovery of this direct C–H bond active coupling process, great interest was aroused toward to wider substrate range and more efficient methods, and encouragingly more complex molecules were synthesized.[17]

However, despite the great advances in the Scholl reaction, the mechanism of the Scholl reaction, which is vital for its optimization, is still not clearly understood. Baddeley first proposed the mechanism of the Scholl reaction, and currently two mechanisms, the arenium cation pathway and the radical pathway, are generally accepted.[18] As shown in Fig. 2, the arenium cation pathway begins with the formation of a σ-complex between a Lewis acid and aromatic compound, which results in the formation of an arenium cation, followed by electrophilic attack, and finally dehydrogenation. In the radical pathway, electron transfer occurs after radical cations are formed, and further lost for the subsequent aromatization. These two mechanisms have been under intense discussion, and in many cases, no sufficient evidence implies that a certain mechanism occurs during the reaction process.

The catalytic system of $AlCl_3$ is a typical system with the requirement of high reaction temperature. Compared with $AlCl_3$ as a reagent, $FeCl_3$ is a more widely used Lewis acid, which is accompanied by mild temperature conditions even in a low-temperature environment. Employing DDQ as a reagent is also a condition of Scholl-type reactions, which is often used in conjunction with sulfonic acid.[19]

It is well known that electron-rich reactants are more likely to follow Scholl-type reactions, and thus this type of reaction is facilitated by the introduction of electron-donating groups or molecules with large conjugate planes. In general, Scholl-type reactions are efficient for building six-membered rings,[20] and in some cases, five-membered and even seven-membered rings were successfully constructed.[21,22] Surprisingly, Scholl-type reactions exhibit selectivity for the formation of multi-membered rings when different reaction conditions are applied to the same reactant.[23]

Iodine-promoted photocyclization reaction. In 1962, Mallory and co-workers discovered a useful photocyclization employing I_2 as an oxidant, rather than O_2, which has become a powerful tool for the synthesis of compounds.[24] It is believed that the mechanism of the Mallory photocyclization undergoes a free-radical process (Fig. 3).[14] When the reactant is exposed to light, a trans-dihydrogen compound is initially produced and it interacts with I_2, resulting in dehydrogenation. Then the

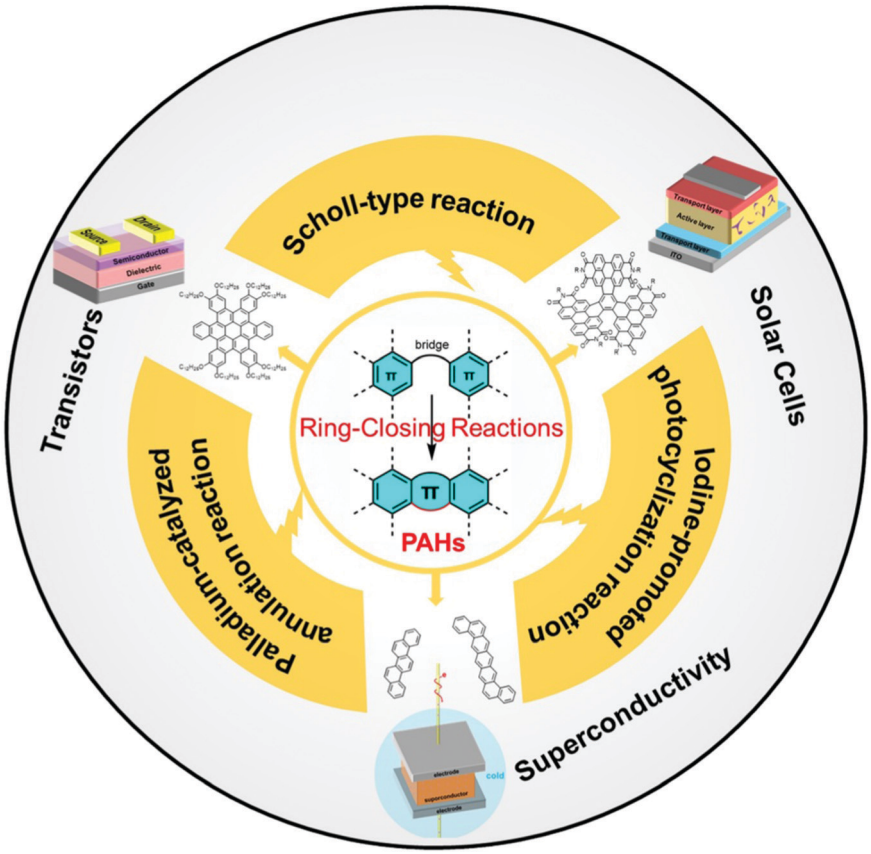

Fig. 1 PAH-based organic semiconductors: ring-closing reactions and optoelectronic device applications.

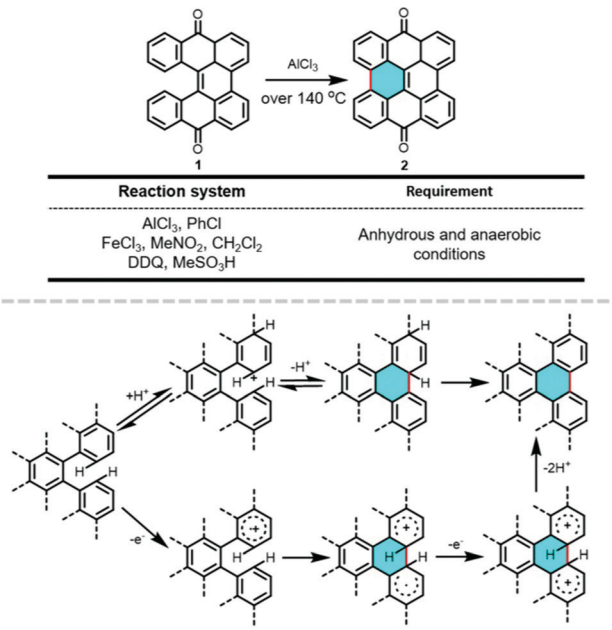

Fig. 2 Scholl-type reaction and its mechanisms.

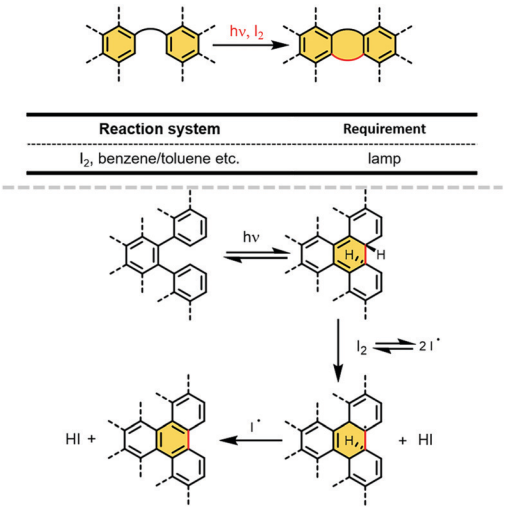

Fig. 3 Iodine-promoted photocyclization reaction and its mechanism.

dehydrogenated species continues to react with the radicals derived from iodine cleavage by photocyclization, resulting in the formation of the target molecules. However, hydrogen iodide, which is formed during this process, is harmful and causes side reactions, and thus, improved conditions have been investigated, such as changing the solvent.

In addition to the requirement of iodine, a light source is necessary to trigger this reaction. For example, mercury lamps are commonly used although sunlight is also capable of initiating the reaction.[25] The reactions can occur under atmospheric

conditions without obvious effects and display wide reactant compatibility.

Palladium-catalyzed annulation reaction. The palladium-catalyzed annulation reaction is essentially an intramolecular C–H/C–X (X = halogen) coupling reaction, which is regarded as a useful methodology to construct PAHs.[16] This reaction requires halogen substitution of the reactant at the ring-closing position. Owning to the difference in bond strength caused by electronegativity, reactions with fluorine-substituted reactants are the most difficult to perform, while iodine-substituted reactants are the most prone to this reaction. Thus, intramolecular C–H/C–F coupling reactions are very rare, and the common reactants are species substituted by bromine or chlorine.[26] The mechanism of this reaction (Fig. 4) proceeds *via* oxidation addition between the halogenated aromatics and palladium catalyst. The intermediate process undergoes a transition similar to the Heck reaction, and finally reductive elimination occurs, resulting in the release of hydrogen halide. Anhydrous and anaerobic conditions are required during the reaction process and the reaction temperature is usually high. In addition, similar to the Scholl-type reaction, this reaction can be employed for the formation of five-membered rings and six-membered rings. It is worth noting that lots of curved molecules, especially those with five-membered rings, are efficiently constructed by this reaction.[27,28] In some cases, reactants with trifluoromethanesulfonic ester (OTf) substitution are also applied to this reaction.

Others. Specifically, this section is about strategies rather than specific reactions. In some cases, such as the requirement of substitution in specific positions, it is rational to form the key aromatic rings in large conjugate molecules *via* multiple reactions in series. This type of method begins by forming a non-aromatic ring connecting the required groups, followed by aromatization (Fig. 5). The Friedel–Crafts cyclization reaction is a simple way to introduce a carbonyl group for the subsequent introduction of substituents, which is convenient and provides a route for the cyclization step. For the aromatization steps, dehydrogenation and nucleophilic addition followed by

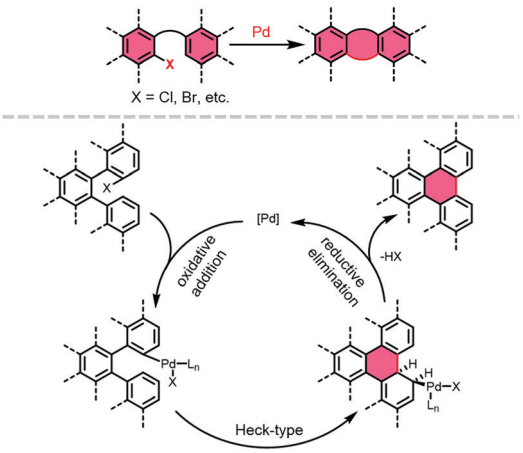

Fig. 4 Palladium-catalyzed annulation reaction and its mechanism.

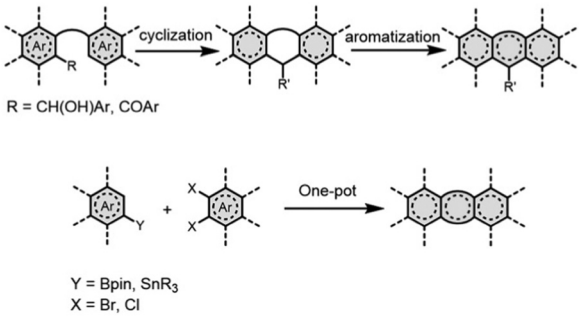

Fig. 5 Examples of other synthesis methods for PAHs.

reduction are alternative ways, which depend on the result of cyclization.

In addition, several efficient one-pot synthetic methods have been developed in recent years for the synthesis of large conjugate molecules.[29–31] These methods are well known as single-step annulative π-extension (APEX) reactions, which efficiently achieve π-extended fused arenes and are regioselective, where they undergo different routes for various regions.[32,33] For the zigzag edges (L-regions) of PAHs, undoubtedly, it is ingenious to employ the concatenation of coupling reactions and annulation reactions. This method requires one reactant to be borate ester and the other to have the character of dihalogen substitution at the ring-formation site.[34] In some cases, a tin reagent and dihalogenated reactant can react, resulting in π-extension of concave armchair edges (bay-regions).[35] We noticed that employing zirconacyclopentadiene for convex armchair edge (K-regions) APEX reactions is also an efficient alternative method, which undergoes double cross-coupling reactions between organometallic reagents and reactants.[36,37]

It is worth noting that on-surface synthesis represents a powerful method for synthesizing larger PAHs, especially those with atomically precise edge structures.[38] On-surface synthesis usually occurs on metal surfaces such as the Au(111) surface and ignores the limitation of solubility of the traditional liquid-phase organic reactions mentioned above. Many complex structures have been efficiently obtained *via* on-surface synthesis, but it is rarely applied due to its low production scale. Also, this method is well summarized in the literature, and thus not discussed here.[39]

2.2. Applications of ring-closing reactions in the synthesis of PAH-based organic semiconductors

PAHs are composed of multiple fused rings and when fused rings form a considerable conjugate plane, the hydrogens of certain sites are relatively reactive, which allows researchers to connect the conjugate plane through the formation of a new aromatic ring. Before the pivotal ring-closing step to build aromatic rings, the common coupling reactions such as Suzuki coupling reaction and still coupling reaction are employed to connect the fragments forming the skeleton of molecules. An early example is the synthesis of perylene.[40] When 1,1′-binaphthalene was treated with $AlCl_3$ at 140 °C, **3** was obtained in low yield, which is an early example of a Scholl reaction. In

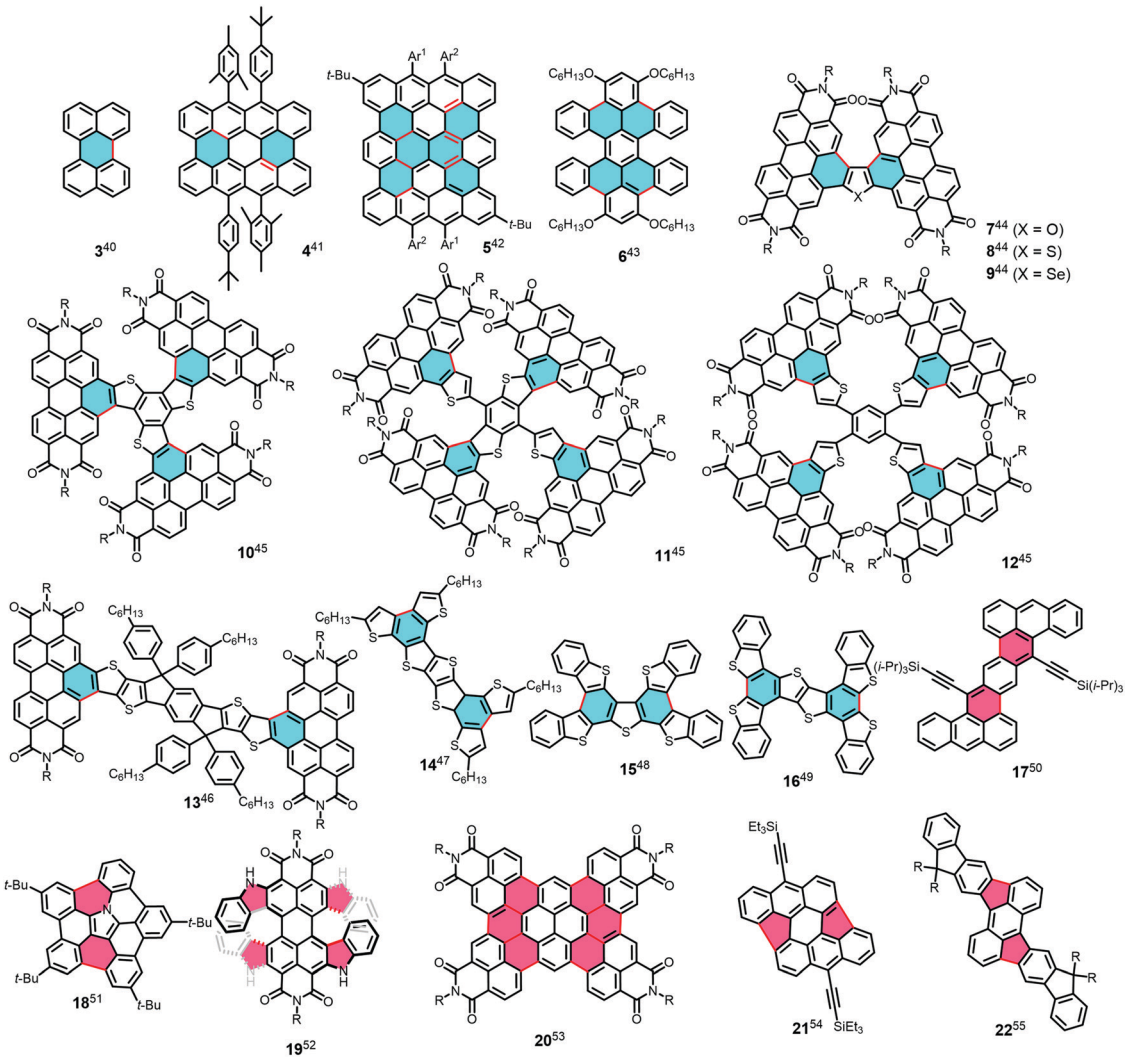

Fig. 6 Chemical structures of the representative PAHs synthesized *via* the above-mentioned ring-close reactions. (For clarity, the rings formed *via* the Scholl-type reaction are marked in blue; the rings formed *via* palladium-catalyzed annulation reaction are marked in pink and the bonds in red represent new constructed bonds.)

2018, **4** was synthesized employing a Scholl-type reaction for the formation of a middle aromatic ring.[41] Under the conditions of DDQ and trifluoromethanesulfonic acid at 0 °C, two aromatic rings were built in one step. Molecule **5**, with a larger conjugate plane than **4**, was constructed and the key ring-closing step occurred in the presence of $FeCl_3$, in which six new C–C bonds were formed simultaneously (Fig. 6).[42] When hexa-phenyl benzene was treated with DDQ/CH_3SO_3H, **6** was obtained through the formation of four C–C bonds instead of producing the corresponding hexa-peri-hexabenzocoronene (HBC).[43]

The bay sites of PDI are active, and thus are usually utilized to expand the conjugated plane. For example, **7** and its derivatives were synthesized following a similar method, which used a nitromethane solution of $FeCl_3$ with unusual heating conditions.[44] High yields exceeding 82% were realized and the different yields were probably because of the different activity of the β-position in thiophene, furan, and selenophen. Yan *et al.* constructed three PDI-based molecules, **10**, **11**, and **12**, by employing Scholl-type reactions after cross-coupling reactions.[45] All three compounds were efficiently obtained in a 2-hour reaction. Molecule **13** was obtained through a cyclization reaction using $FeCl_3$ at 50 °C from the product of the Stille coupling reaction. After the 8 h reaction, the yield of **13** reached up to 80%.[46] Hu *et al.* reported a series of fused-thiophene compounds, **14**, **15** and **16**, which were synthesized from the precursor with thiophene or benzothiophene linked to the aromatic core through a Scholl-type reaction catalyzed by $FeCl_3$.[47–49]

The skeleton of **17** was built through the key Pd-catalyzed intramolecular Heck reaction.[50] The reaction removed hydrogen halide to form C–C bonds at 160 °C, but the yield was only 27%. A buckybowl-shaped molecule, **18**, with embedded nitrogen, was realized by Shinokubo *et al.*, employing a palladium-catalyzed annulation reaction for the coupling of two C–C bonds in 46% yield to form a distorted buckybowl.[51] Another distorted structure, **19**, embedded with two heterohelicenes was furnished by four-fold C–H/C–Br coupling between PDI and the bridging

benzene in the presence of $Pd(OAc)_2$ and P^tBu_3 HBF_4, resulting in the formation of four five-membered rings.[52] Surprisingly, Würthner *et al.* reported that **20** was obtained in a one-pot reaction, which actually connected the Suzuki coupling reaction with the Pa-catalyzed annulation reaction successfully.[53] It is worth mentioning that **20** was not obtained when utilizing a Scholl-type reaction due to this electron-poor system. **21** is regarded as a fragment of C_{70} and the curve of **21** is derived from the formation of two five-membered rings, which were built through palladium-catalyzed annulation reaction with $PdCl_2(PPh_3)_2$ as the catalyst at 160 °C.[54] Molecule **22** also contains two five-membered rings and these key rings were synthesized *via* palladium-catalyzed annulation reaction in a Schlenk tube.[55]

Fagnoni *et al.* synthesized **23** by employing photocyclization, where careful optimization of the conditions led to the maximum yield of 93% under 310 nm lamp irradiation.[25] Another linear acene, **24**, extended along the ortho-orientation was produced *via* photocyclization and isolated as a byproduct.[56] Actually, many HBC-based molecules can be synthesized *via* photocyclization and are also synthesized through this method, which forms multi rings as the key step. For instance, when the precursor was treated with a propylene oxide solution of I_2 under light, **25** was obtained in 70% yield.[57] Furthermore, **26** was prepared following the same procedure using the product of a condensation reaction.[58] Molecule **27** with a larger conjugate plane compared with **25** was prepared following the same photocyclization process, leading to the formation of six aromatic rings.[59] Some key monomers of polymers can be obtained *via* photocyclization. Facchetti *et al.* achieved the synthesis of **28** and the critical fragment of thiophene-incorporated PDI was synthesized under photocyclization conditions.[60]

Benefitting from the activity of the bay hydrogen, numerous PDI-based molecules with unique structures have been efficiently constructed *via* iodine-promoted photocyclization reactions after simple coupling reactions.[61] For the synthesis of molecules **29–41** (Fig. 7), the step of photocyclization was

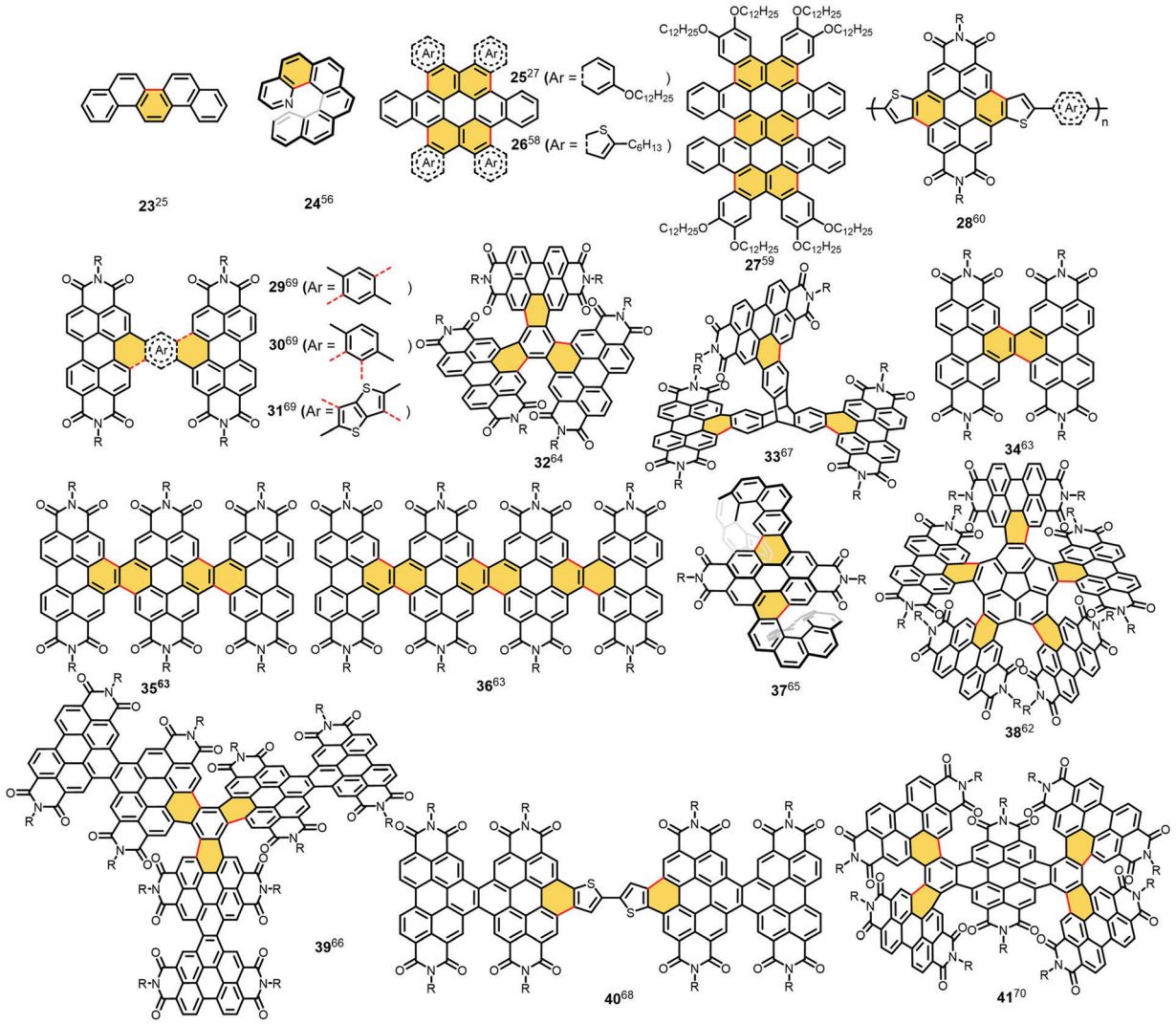

Fig. 7 Chemical structures of the representative PAHs synthesized by above-mentioned ring-close reactions (rings formed *via* iodine-promoted photocyclization reaction marked in yellow; the bonds in red represent new constructed bonds).

similar but some molecules that are difficult to form rings and affected by the distorted structure require heating conditions to promote the reaction.[62–70] Referring to the preparation of molecule **42–44**, the strategy of combining two reaction steps was applied, which began with Friedel–Crafts alkylation reaction, followed by dehydrogenation.[71–73] Accordingly, **45–47** were achieved *via* combined strategies but the diketone product after Friedel–Crafts alkylation reaction required two steps, nucleophilic addition and reduction reactions with $SnCl_2$, to arrive at the target molecules.[74–76] It is worth noting that the strategy of combining addition and reduction reactions is appropriate for five-membered rings formed by the Friedel–Crafts alkylation reaction (Fig. 8), where **48** is an example of this.[77] The key five-membered rings of molecule **49** were yielded by a method similar to **42** but intramolecular Friedel–Crafts reaction occurred on the ester group.[78] For the synthesis of **50**, after Friedel–Crafts cyclization, the key helical structure was formed, and then oxidative dehydrogenation gave the final product.[79] A series of molecules, **51–54**, reported by Mastalerz *et al.* was easily obtained *via* a one-step two-fold condensation between bridged methylene and aldehyde groups from the products of coupling.[80] Both Scholl-type reaction and the aforementioned strategy combining two reaction steps were employed to produce molecules **55** and **56**.[81,82] Two five-membered rings and two seven-member rings are formed in **55**, while two five-member rings and two six-member rings are formed in **56**. The two rings on the right half of molecule **57** were constructed by photocyclization reaction, whereas subsequently the two rings on the left half were synthesized by employing a Scholl-type reaction catalyzed by $FeCl_3$.[83] **58–60** were prepared *via* multiple ring-closing reactions, which have different reaction conditions from that mentioned previously such as ICl/dichloromethane and KOH/quinoline.[84–86] For **58** and **59**, the first ring-closing reaction was followed by the introduction of substituents, and

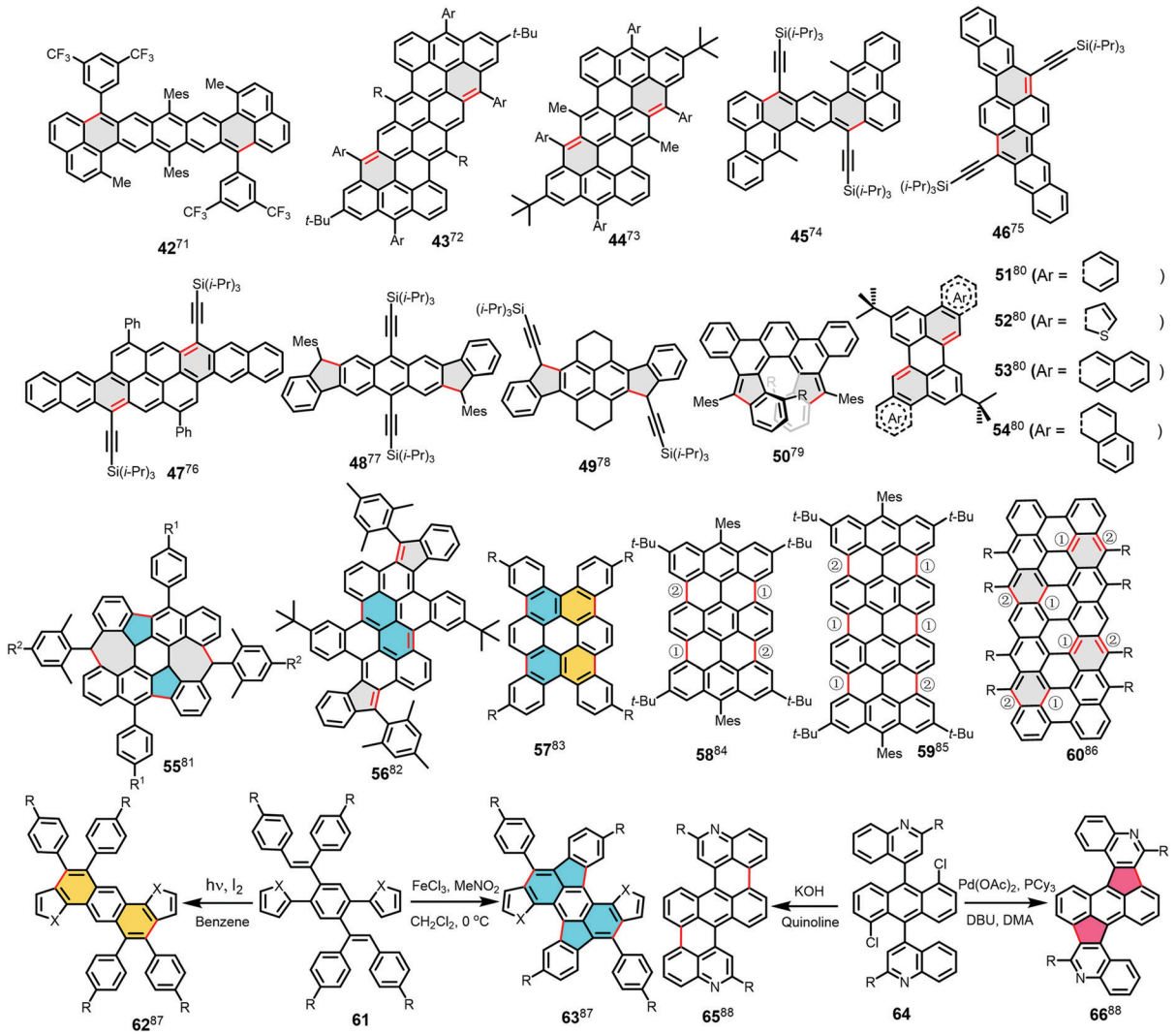

Fig. 8 Chemical structures of the representative PAHs synthesized *via* the above-mentioned ring-close reactions. (For clarity, the rings formed *via* Scholl-type reaction are marked in blue; the rings formed *via* palladium-catalyzed annulation reaction are marked in pink; the rings formed *via* iodine-promoted photocyclization reaction are marked in yellow; and the rings formed *via* other methods are marked in gray. The bonds in red represent new constructed bonds. The serial number beside the bonds indicates the order in which the bonds are formed.)

then another ring-closing method was applied, producing the final products. When ICl-induced benzannulation reaction was carried out the during synthesis of molecule **60**, intramolecular cyclodehydrogenation occurred simultaneously. Subsequently, substituents were introduced through the combination of addition reaction and intramolecular Friedel–Crafts cyclization.

Huang *et al.* reported that when reactant **61** was treated under the conditions of the Scholl-type reaction, six-membered rings and five-membered rings were simultaneously formed.[87] However, only six-membered rings were built employing the condition of photocyclization reaction to obtain molecule **62**. Nitrogen-containing molecule **66**, similar to **63** in structure, was obtained *via* palladium-catalyzed annulation reaction by removing hydrogen chloride.[88] Also, when KOH and quinoline are present in the reaction system, **65** is achieved, resulting from the formation of two six-membered rings. The above-mentioned two examples illustrate the differences in the different ring-closing reactions for the formation of rings, which imply that the selection of the ring-closing method is significant.

2.3 Functionalization of PAH-based semiconductors

Although the materials synthesized through ring-closing reactions possess abundant properties, functionalization is considered an excellent approach for endowing materials additional properties. Firstly, alkyl chain substitution is a widely used method to enhance the solubility of materials.[89,90] Due to the large, rigid, conjugate plane, most materials become insoluble after ring-closing reactions.[91] Hence, the introduction of alkyl chains is not only necessary but also results in extra properties such as controllable assembly.[92] Molecules **67** and **68** are good examples, which both can assemble into nanotubes.[93,94] This type of alkyl chain includes alkoxy chains and fluorine alkyl chains (Fig. 9).

Halogen substitution is also a classic strategy and acts more on energy levels and stacking modes of materials, even changing the transport type. For instance, phthalocyanine copper manifests a certain p-type character, whereas perfluorophthalocyanine copper exhibits n-type transport property.[95] The influence on molecular accumulation can be reflected in molecules **69** and **70**.[96,97] It is worth noting that both the alkyl chain and halogen substitution do not occur directly on molecules that have undergone ring-closing reactions. In most cases, the precursor molecules already have a substitution from functionalization, and then form the backbone of the target molecules through the ring-closing reactions, which highlights the importance of molecular design.

Introducing diimide groups is sufficient to change the energy levels and transport properties. PDI and NDI are typical representatives of this type of material. However, the process of imide introduction is complex, time-consuming, and results in low yield. Zhen *et al.* reported the facile synthesis of aromatic diimides *via* a one-pot reaction in moderate yield.[98] This approach was established for palladium-catalyzed carbonylation, which employed tetrabromo aromatic molecules and a CO carbon source. A wide range of reactants are capable of undergoing this reaction with a moderate yield, which demonstrates the broad applicability of this reaction. Thus, this method provides a solid foundation for functionalization through the introduction of imides.

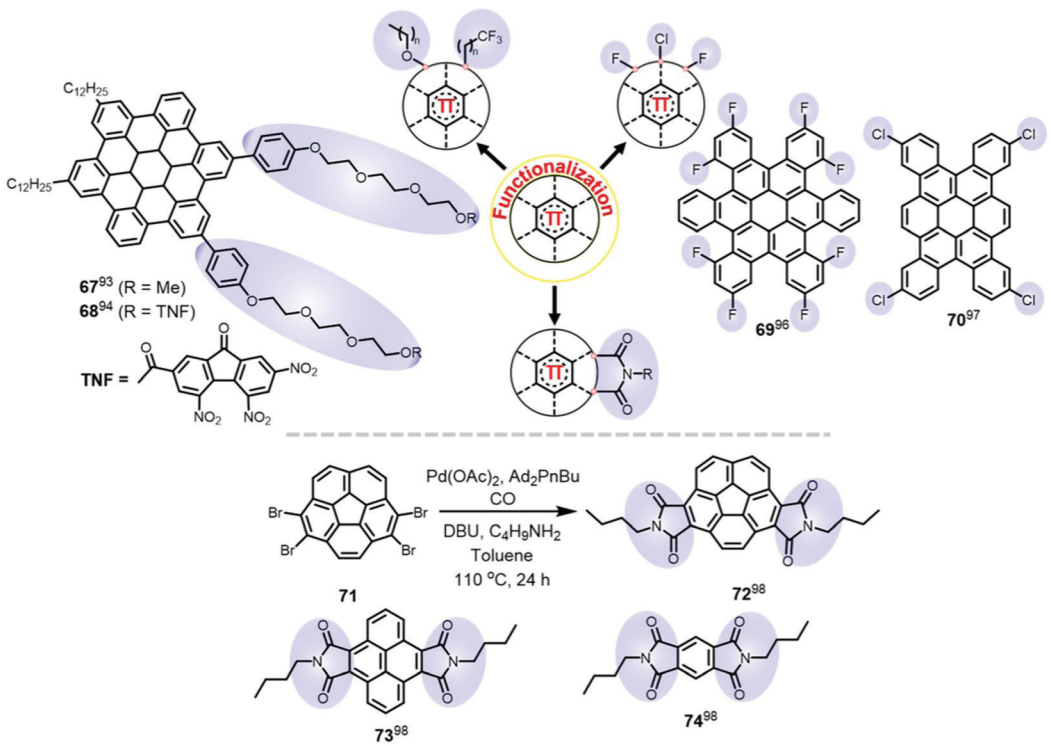

Fig. 9 Three synthetic routes for the functionalization of PAHs and their representative derivative molecules.

In addition, heteroannulation at a specific site is a promising strategy to further optimize the structure of molecules.[99,100] In particular, the heteroatoms S and Se are incorporated at the bay regions of PDI-based molecules, which strengthen the inter- and intramolecular interactions.[101]

3. Device applications of PAH-based semiconductors

3.1. Organic field-effect transistors

OFET are the cornerstone of organic electronics, which have great potential for applications in flexible organic circuits, wearable devices, biological electronics, *etc.* The development of high-performance OFET devices is crucial for their applications in various fields.[102–104] For these three-terminal devices, the organic semiconductor layer is the key component affecting the performance of OFETs, which is responsible for the transport of charge carriers. According to the current understanding and recognition of the charge transport process and mechanism in organic semiconductor materials, larger transfer integrals and more efficient charge transport can be obtained with a large intrinsic conjugated structure and compact molecular packing mode in the aggregation state, which is beneficial for achieving high-performance OFET devices.[3,105] Materials based on PAHs consist of multi fused rings, which guarantee their extended conjugate structure and good compact packing in the aggregation state due to strong intermolecular interactions.[1] Thus, PAH materials display promising applications in OFETs. Furthermore, their unique molecular structure endows them with new properties such as chirality and radical character, which will be discussed below (Fig. 10).

High-mobility OFETs. PAHs as a typical class of organic semiconductors have been widely used in OFETs. Perylene is a commercially available material with a minor conjugated plane containing five fused benzene rings. It has been found that two crystalline phases, the α-phase and *β*-phase, exist in the perylene crystal. Wang *et al.* reported a study on the OFET performance of different crystal phases based on **3**.[106] The droplet pinned crystallization (DPC) method was employed, resulting in mixed-phase crystal arrays. The X-ray diffraction study indicated that the α-phase and β-phase adopted the typical sandwich-herringbone packing and herringbone packing, respectively. Thus, the α-phase provides a more effective charge-transport channel, resulting in higher mobility. In the case of a bigger conjugated plane, a surprising stacking phenomenon is observed. For example, **25** and derivatives are one type of materials with large aromatic cores, the so-called ''super-benzene'', and owing to their strong π–π interaction, this type of material exhibits the tendency to organize into columns, which implies excellent intrinsic carrier mobilities.[107] Müllen and co-workers focused their efforts on the synthesis of HBCs and plenty of methods have been developed to optimize the self-assemble process to form one-dimensional column stacks. Although their mobility was not very high, as expected, a deep understanding of this type materials and pioneering methods were well established.[108]

Nuckolls *et al.* reported that with octa-substituted alkoxyl side chains, **25** underwent a self-assembly process, organizing into fibers.[57] The resulting oriented long-range order fibers were further measured for their OFET performance and their hole mobility was determined to be about 0.02 $cm^2\ V^{-1}\ s^{-1}$. Different properties in shape and electricity were found as the HBC-based molecular plane was further expanded. Firstly, **27** displayed a distorted conformation owing to steric hindrance, which is a shape complementary to $PC_{70}BM$. Alternatively, **27** treated by acids underwent protonation, and then charge-transfer reactions under anaerobic conditions, which constructed doping thin-film transistors with switch-off ability through a gate bias.[59]

Functionalization of HBC-based molecules is a promising strategy to adjust the macroscopic properties of materials. For instance, Loo *et al.* confirmed that the crystallization of particular polymorphs was regulated by fluorination.[109] When chlorine-substitution was employed, co-facial packing was exactly adopted by a derivative of **27** presumably due to intermolecular Cl···Cl interaction.[96] However, the thin-film transistor of **27** derivative only exhibited a mobility of up to 0.24 $cm^2\ V^{-1}\ s^{-1}$, which was lower than that of the parent HBC. With tetraalkoxy substitution, the HBC-based molecule possessed stimulus response character when employing single-walled carbon nanotubes as point contacts for constructing OFETs (Fig. 11a).[110] Columnar nanostructures were formed though self-organization, which are composed of molecular stacking with an orientation parallel to the conducting channel. Thus, efficient charge transport was realized, and surprisingly photocurrents with a larger on/off ratios were detected when the devices were exposed to light. By regulating the side chain

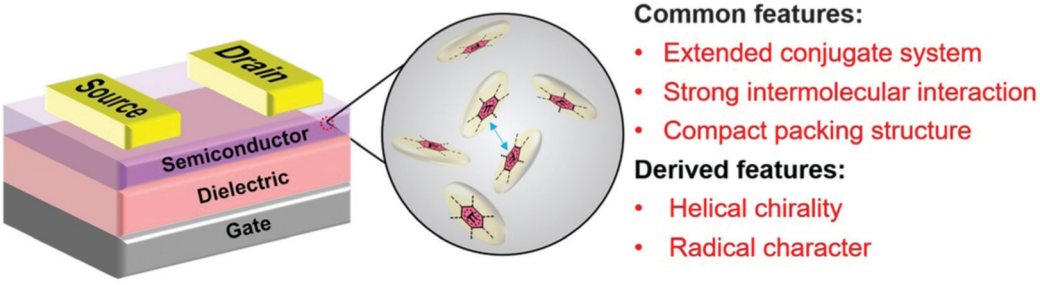

Fig. 10 Schematic of OFETs and the unique features of PAH-based materials for the semiconductor layer in OFETs.

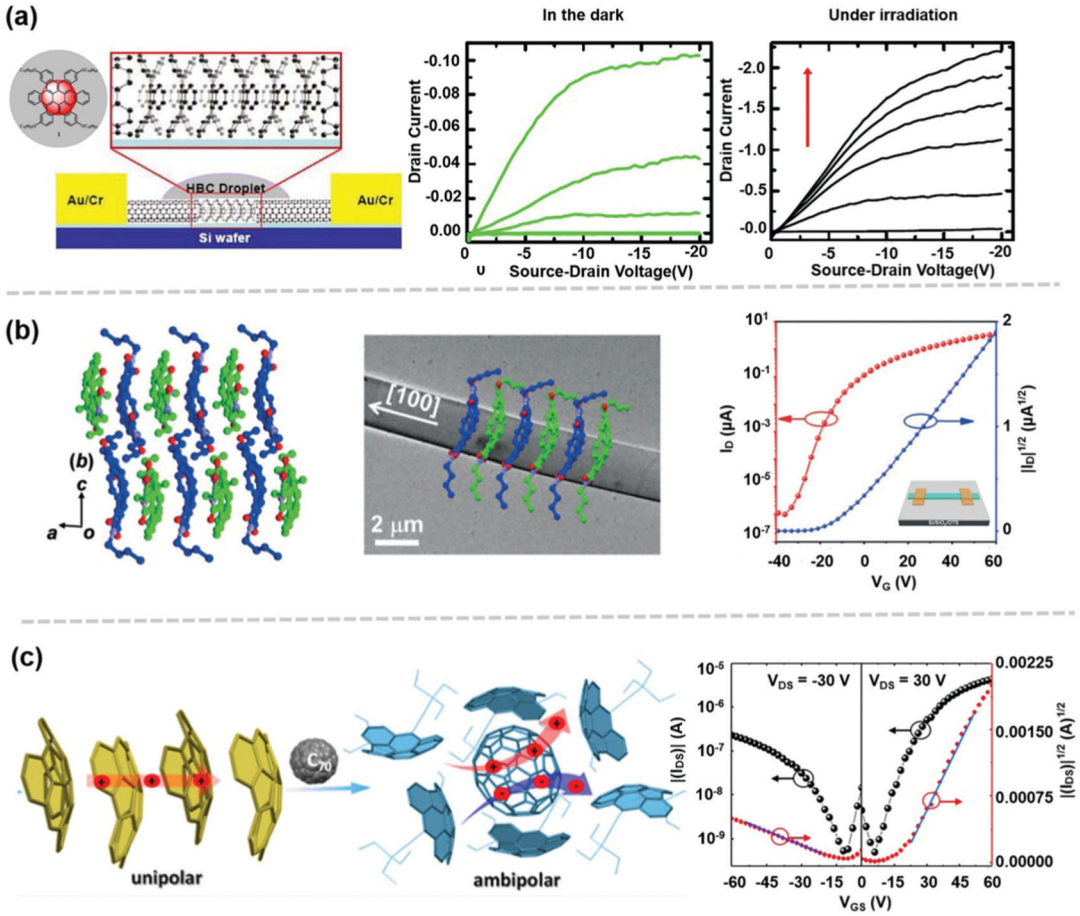

Fig. 11 PAH-based OFETs. (a) Photoresponsive transistors based on monolayer films of HBCs. Reprinted with permission from ref. 110. Copyright 2009, the National Academy of Sciences of the USA. (b) Functionalization of corannulene and its application in n-type OFETs. Reprinted with permission from ref. 98. Copyright 2020, Wiley-VCH Verlag GmbH & Co. KGaA, Weinheim. (c) OFETs based on cocrystal assembly by C_{70} and 17 for ambipolar transport properties. Reprinted with permission from ref. 54. Copyright 2020, the American Chemical Society.

of HBC-based molecules, other various functional devices can be constructed such as chemoresponsive transistors.[111]

Functionalization not only results in the promotion and optimization of properties, but also regulates the energy level of materials, leading to a change in their transport characteristics. For instance, the functionalization of corannulene with imides resulted in a lower LUMO energy, down to −3.10 eV, compared with that of corannulene. The molecule underwent one-dimensional slipped stacking and microcrystals growing along the direction of stacking were obtained, which implied an efficient transport performance (Fig. 11b). Finally, n-type behavior based on this material was achieved with a mobility of 0.05 $cm^2 V^{-1} s^{-1}$.[98]

The excellent properties of HBC-based molecules originate from the core coronene to a large extent. Thus, the modification of coronene is a useful strategy to tune its photoelectric properties. Wu *et al.* first reported a new family of 1,2,3,4,7,8,9,10-tetrabenzocoronenes (TBCs), and the average hole mobility was up to 0.61 $cm^2 V^{-1} s^{-1}$ for **57** by using the space-charge limited-current (SCLC) technique.[83] Three TBC derivatives with different substitutions were investigated for OFETs by Tao *et al.* and it was observed that the packing mode varied for the different substitutions, which suggested that a shifted π–π stacking was adopted by that with methyl substituents and the others all exhibited co-facial π–π stacking.[97] Due to the 1D growth together with stacking, the organic single-crystal field-effect transistors (SCFETs) of **57** with chlorine-substitution gave the highest mobility among them of up to 0.7 $cm^2 V^{-1} s^{-1}$. Tao's group further reported the effect of substituents on the crystal packing and properties of **57**, which indicated that the unsymmetrical hexa-fluorinated molecule delivered a mobility as high as 1.19 $cm^2 V^{-1} s^{-1}$ on account of its slightly shifted π–π stacking.[112]

Co-crystallization engineering has been regarded as an effective strategy towards improving the properties of a single component and bringing about unpredicted chemicophysical properties, which is especially beneficial for building multifunctional and high-performance optoelectronic devices.[113,114] Generally, organic cocrystals are assembled through noncovalent intermolecular interactions, such as halogen and hydrogen bonds, π–π interaction and charge transfer interaction. Bowl-shaped PAHs are viewed as a fragment of fullerene, which is complementary to buckybowls, and thus possess potential to crystallize with buckybowls.[51,115] Zhang *et al.* found that when **21** was employed as the electron donor to crystallize with C_{70}, a

two-dimensional cocrystal was well obtained (Fig. 11c).[54] The resulting cocrystal displayed ambipolar transport with hole and electron mobilities of up to 0.07 $cm^2 V^{-1} s^{-1}$ and 0.40 $cm^2 V^{-1} s^{-1}$, respectively. The hole mobility was higher than that of the sole component **21**, which illustrates the high potential of cocrystals for constructing organic devices based on novel semiconductors. Besides, cocrystals allow the possibility of realizing photoelectric integrated devices and other functional devices through the synergy of multiple components.[116,117]

Chiral OFETs. Generally, linear acene is planar but with an increase in the number of ortho-fused rings, unexpectedly the molecular plane curves upward along a spiral due to steric hindrance. This architecture endows helicenes a special nature, namely chirality, even though no asymmetric carbons or other chiral centers exist in its structure.[118] For so-called helicenes, the left-handed helix (denoted as (M)) and right-handed helix (denoted as (P)) correspond to levorotatory and dextrorotatory, respectively. This chiral architecture delivers peculiar chiroptical properties containing optical rotatory power and circular dichroism, which further provoke broad applications in quantum optics, optical spintronics, *etc.*[119]

Helicenes possess multiple possibilities for structural expansion to adjust their properties, such as forming chiral nanographenes.[120] Indeed, there are a few examples of the application of helicenes in optoelectronic devices. In 2013, Campbell *et al.* reported that an N-incorporating helicene formed well-ordered crystallized domains after annealing and behaved as a p-type material when employed in OFET.[121] The circularly polarized light responsivity based on enantiomeric helicene FETs was investigated and a highly specific photoresponse was achieved, which is related to the handedness (Fig. 12b).

PDI has become a popular unit with excellent optical and electrical properties and it is envisaged that integrating PDI and helicenes into one molecule will produce a structure that has the characteristics of both parents (Fig. 12a). Wang *et al.* demonstrated that with two merged [6]helicene structures, **37** possessed excellent chiroptical responses in both absorption and emission, which exhibited dissymmetry factors $|g_{abs}|$ of 0.012 and $|g_{lum}|$ of 0.002, respectively.[65] Although several types of these structures have been developed, it is worth noting that a trade-off should be considered for their application, where planar π-systems are required for electrics, while a distorted π-system is demanded for chirality and strong coupling with circularly polarized light.[122] Lin *et al.* discovered that **19** inherited high dissymmetry factors and high mobility from the parent helicenes and PDI.[123] Surprisingly, with *ortho*-π-extension, its absorption was shifted to the near-infrared (NIR) region, and ambipolar charge transport was obtained. Benefiting from these properties, organic phototransistors were

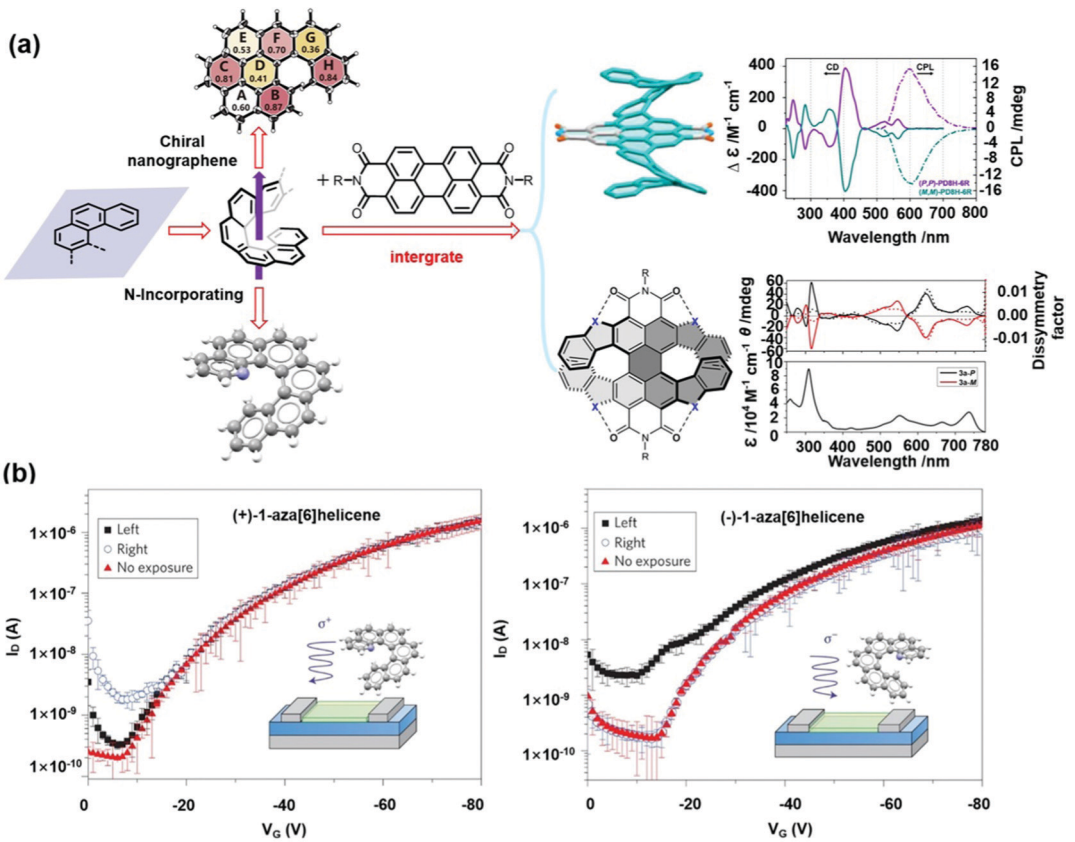

Fig. 12 PAH-based chiral OFETs. (a) Extension of chiral structure of helicene. Reprinted with permission from ref. 65. Copyright 2020, the American Chemical Society. (b) Chiral transistor and its photoresponse property. Reprinted with permission from ref. 121. Copyright 2013, Nature Publishing Group.

constructed, which displayed high photoresponsivity and high external quantum efficiency under NIR light irradiation.

Biradicaloid-based OFETs. Most PAHs exhibit closed-shell electronic features in the ground state. While in the process of synthesizing various PAHs, it has been found that some target molecules have very high reactivity and no signal peaks appear in their NMR spectra at room temperature, which is attributed to their intrinsic diradical properties with an open-shell structure. With further research, these types of materials are usually accompanied by a narrow singlet–triplet gap, ambipolar character, *etc.*, endowing them great potential applications in the fields of organic spintronics, organic magnets, singlet splitting, and nonlinear optics.[124] Phenalenyls is a typical type of system developed and charactered by Nakasuj and Kubo *et al.*, which possess singlet biradical properties in the ground state.[125–127] This inspired the search for biradical species and it is believed that the zigzag-edged zone of graphene nanoribbons is prone to generate radical character, and thus tremendous efforts have been focused on the synthesis of graphene-like molecules with zig-zag edges to obtain biradical species. However, the main challenge is their intrinsic instability for applications.[77] Thus, to overcome this issue, bulky or electron-withdrawing groups are introduced at strategic positions, such as mesityl. Alternatively, the biradical character y is considered, which is a reflection of the physical properties of open-shell singlet biradicaloids. Therefore, it is expected that species with both stability and large y can be obtained, and therefore, it is essential to understand the structure-stability-biradical character relationship.

The so-called [*n*,*m*]-peri-acenes, which are comprised of *m* rows of peri-fused [*n*]acenes, possess rich zigzag edges, and thus are an ideal model for biradical character.[128] The structure–property relationship of biradical species is well reflected by the [*n*,*m*]-peri-acene platform. The minor peri-acene, bisanthene, was reported by Clar with a small biradical character *y* (0.07), and higher biradical character was obtained through enlarging the conjugate system of bisanthene horizontally and vertically.[41] As shown in Fig. 13a, the biradical character

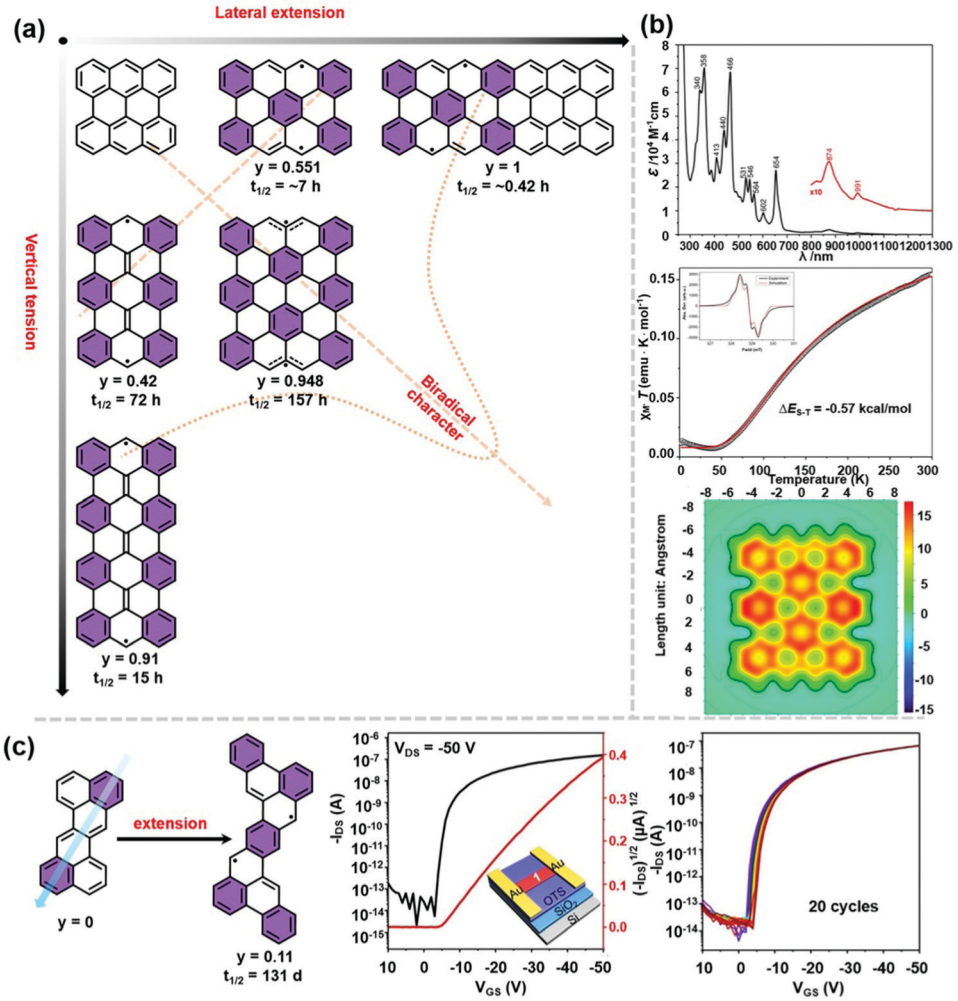

Fig. 13 PAH-based biradical molecules and their properties and OFETs. (a) Extended structure and characters of biradical species. (b) Characterization of biradical features. Reprinted with permission from ref. 42. Copyright 2020 Wiley-VCH GmbH. (c) OFETs based on biradical species and their properties. Reprinted with permission from ref. 74. Copyright 2021, Wiley-VCH GmbH.

increased significantly with an increase in the degree of conjugation, no matter in the horizontal or vertical direction. However, the half-life time of these materials presented a decaying trend, which indicates a reduction in their stability. However, **5** is an exception, which is possibly because most of its active sites are occupied by large hindrance groups.[42] Furthermore, the systematic characterization of the properties of the stable diradicaloid was performed using Vis-NIR absorption spectroscopy, electron paramagnetic resonance (EPR) spectroscopy and isochemical shielding surface (ICSS) mapping (Fig. 13b). It is obvious that multiple intense absorption bands in the visible spectrum range and a weak absorption band in the NIR region were present in the absorption spectrum of **5**, in which the latter originated from the low-lying singlet excited state. The radical signal was clearly displayed in the ESR spectra and based on the SQUID measurement of **5**, the ΔE_{S-T} value of -0.57 kcal mol^{-1} was obtained. The eight localized aromatic sextets existing in **5** were uncovered by the 2D ICSS map, which was helpful to understand the diradical site.

Zethrenes are considered as candidate biradical species, which consist of head-to-head splicing of phenalenyl units to some extent. Stretching along the zethrene molecular skeleton is another strategy for obtaining biradical species.[129] Recently, Sun *et al.* constructed air-stable OEFTs based on **45** (Fig. 13c). The peak signal in the ESR spectra confirmed the presence of paramagnetic species due to the diradical character and the signal intensity decreased with a decrease in temperature, which implied the character of the diamagnetic singlet ground state. The SCFETs of **45** exhibited a hole mobility of up to 0.15 cm^2 V^{-1} s^{-1} under ambient conditions; meanwhile, the devices possessed considerable bias-stress stability and storage stability.

The radical character of many molecules results from the change in the aromatic quinone structure in PAHs. It is well known that the introduction of defects not only opens the band gap of graphene, but also changes its optical, electrical and magnetic properties. Even more remarkable, biradical character is observed in nanographene with defective structures.[130,131] Indenofluorenes and their π-extended derivatives provide support for the deep understanding of biradical character in defective structures.[132] For instance, Haley *et al.* developed a new species **48** intercalated by a five-membered ring, which possessed remarkable stability and open-shell character. The fundamental OFET devices, constructed by the film of **48**, yielded a balance ambipolar transport with a hole mobility of 2×10^{-3} cm^2 V^{-1} s^{-1} and electron mobility of 4×10^{-3} cm^2 V^{-1} s^{-1}.[77] Furthermore, replacing the aromatic ring on the periphery in indenofluorenes also generates biradical species with considerable biradical character, such as thiophene-integrated species.[133] Surprisingly, the rational design of helical arenes endow them with biradical character. Wu *et al.* illustrated the successful integration of biradical character and helicenes. Benefiting from the helical structure and biradical character, compound **50** not only presented chiral features, but also delivered ambipolar transport behaviors.[79]

3.2. Organic solar cells

Organic solar cells (OSCs) are promising energy-harvesting devices and have great potential for wide practical applications due to their light weight, soluble processing, low cost, low pollution, *etc.*[134] In recent years, rapid development has been achieved in OSCs, especially devices constructed using non-fullerene acceptors. For instance, Zhan *et al.* discovered a new acceptor, ITIC, based on a fused-ring core, which broke the limit of the fullerene acceptor.[135] In 2019, Zou *et al.* reported a record efficiency employing Y6 as an acceptor.[136] These examples imply the advantages brought by fused-ring electron acceptors. Composed of multi fused-rings, PAH materials present a wide absorption spectrum accompanied with strong adsorption in the visible light region due to their large conjugate structures, which have an effect on various indexes of OSCs, resulting in high performances (Fig. 14). In addition, PAH materials produce a spatial structure to suppress strong self-aggregation, benefiting from their blend morphology, which leads to high performances. This is in contrast to the intensive aggregation expected in OEETs, implying the excellent adaptability of PAH materials. A detail discussion of their applications in OSCs is presented below.

The power conversion efficiency (PCE) is the most important parameter in organic solar cells, which determines whether they can be used for practical applications. Therefore, continuing efforts are devoted to increasing the PCE. Generally, OSCs are composed of electrodes, a transport layer, and active layer, where among them, the most important is the active layer. To obtain a high PCE, it is essential to focus on the active layer and its

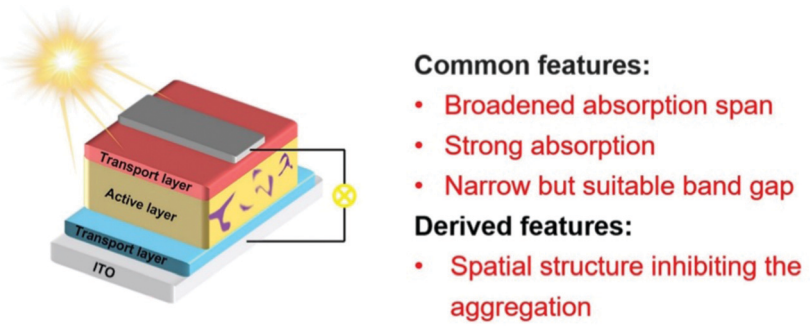

Fig. 14 Schematic of OSCs and the unique features of PAH-based materials as the active layer in OSCs.

constituent materials. The active layer is a binary system, consisting of a donor and acceptor, or multiple systems, where a photocurrent is generated. A high PCE is guaranteed by the positive coordination between the donor and acceptor. The physical processes of OSCs include light absorption, exciton generation, exciton diffusion, and exciton dissociation, where excitons are regarded as Coulombically bound electron–hole pairs.[137] Before any further discussion, it is vital to realize that the performance of OSCs depends heavily on the chemical structure of their donor and acceptor molecules. The PCE is determined by the open-circuit voltage (V_{oc}), short-circuit current (J_{sc}), and fill factor (FF) as the product of three parameters, and these three parameters are closely related to both the donor and acceptor structure. Firstly, as a device that absorbs sunlight and then converts it to electricity, absorption in the full visible region, as much as possible, is a prerequisite to ensure effective exciton generation and exciton dissociation, which strongly affect J_{sc}. Consequently, the complementary absorption of the donor and acceptor must cover the visible region as much as possible. However, the absorption of the donors is limited, and thus molecules with a large conjugate plane are necessary due to their broadened absorption. Alternatively, carrier transfer is required in the active layer, and the HOMO of the donor material needs to match the LUMO of the acceptor for carrier transport. This energy difference has an effect on V_{oc}, which indicates that the donor and acceptor should be carefully selected.[138] Moreover, the carrier mobilities of the donor and acceptor materials affect the FF, which depends on the efficient extraction of carriers produced by light. In the active layer, the FF can be improved by the existence of crystalline or relatively pure aggregation domains, which meets the demand for the active layer. In fact, regulating the morphology of the active layer is the most complex and common issue in OSCs. For optimal device efficiency, it is believed that nanoscale phase separation is required, which can balance efficient carrier generation and inhibition of recombination.[137,139] Briefly, adjusting topography is overall engineering, which requires many factors to be comprehensively considered.[140]

In 2014, Nuckolls *et al.* employed different donors to build devices with **34** as the acceptor, where the two donors exhibited different absorption.[141] The results demonstrated that the

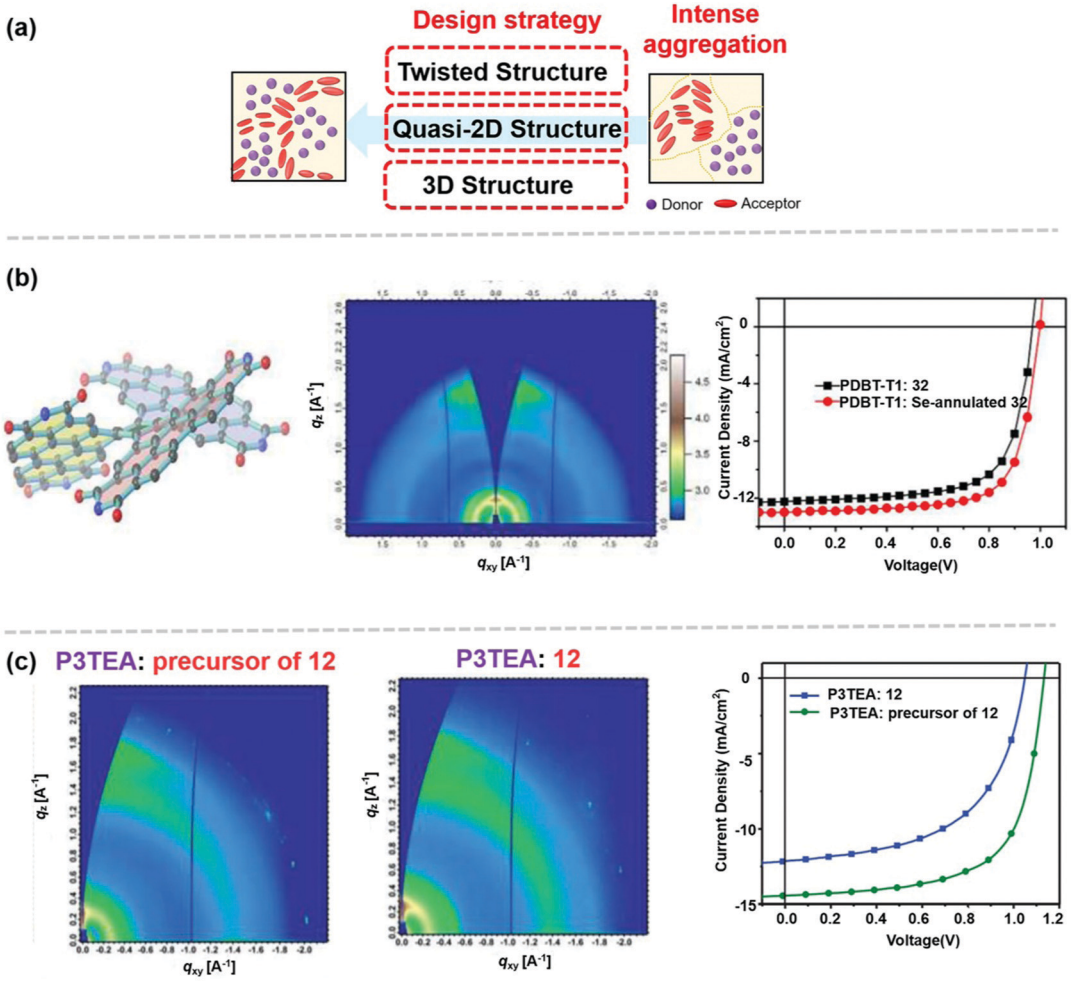

Fig. 15 PAH-based OSCs. (a) Molecular design strategy for PDI-based acceptor. (b) Molecular shape, 2D-GIWAXS patterns and performance of **23**. Reprinted with permission from ref. 64. Copyright 2016, the American Chemical Society. (c) 2D-GIWAXS patterns and performance of **12** and its precursor. Reprinted with permission from ref. 45. Copyright 2018, Wiley-VCH Verlag GmbH & Co. KGaA, Weinheim.

systems with more complementary spectra presented a higher PCE in the absence of additives. This is because the J_{sc} becomes larger due to the more complementary spectrum of absorption, corresponding with the previous understanding. PDI-based non-fullerene acceptors have also found application in solar cells.[142] Many of them are π-expanded rather than monomers, which results in wide absorption for adapting their applications in OSCs.[142,143] Molecules with a large conjugated plane, such as PDI, possess strong self-aggregation ability due to their intermolecular π–π interaction, which is beneficial for OFETs but is disadvantageous in OSCs. This issue leads to unfavorable large-scale phase separation, which is usually accompanied by low PCE.[67] Thus, to alleviate the issue, several strategies for the design of molecules have been proposed including twisted structure, so-called quasi-2D structure and 3D structure (Fig. 15a). All three strategies, essentially, result in structural distortions in the molecules to inhibit their self-aggregation. Jen *et al.* illustrated that the geometry of **8** showed distortion with a twist angle of up to 27.2°.[44] Then OPVs were constructed by selecting PTB7-Th as the donor and an average PCE of 5.69% was achieved. AFM analysis clearly demonstrated that favorable phase separation was realized, resulting in positive FF. Besides, compared with **8**, the molecule before the ring-closing reactions exhibited a lower PCE with a low J_{sc}, which was partly attributed to the different absorptions in the short wavelength region. This confirms that the broad absorption originating from the large conjugate plane is beneficial to the performance of the devices.

In fact, in the so-called quasi-2D structure, the rigidity of the molecule offsets the adverse effects of the distorted structure on its transport performance. Zhang *et al.* investigated the device performance of **40**, which presented a PCE of 5.89%.[68] Although the quasi-2D structure did not work as well as expected, balanced carrier transport was realized. The AFM images of both the blend film of **40** and its precursor exhibited decent miscibility and morphology compatibility, and therefore their FF were similar. The unexpected low performance was on account of the strong bimolecular recombination and unfavorable packing properties in the blend film.

In 2016, Wang *et al.* explored the three-bladed propeller-shaped molecule **32**, the crystal of which showed a compact 3D network assembly. It was employed as an acceptor to build an OSC and a considerable PCE was obtained due to its comprehensive performance such as broad absorption and good film morphology (Fig. 15b).[64] When DIO was further employed for optimization, the donor in the blend film tended to adopt a face-on orientation, resulting in an improved performance. Selenium-annulated functionalization was used to improve the performance and the results were promising with a PCE of up to 8.05%. Further, with the modification of the additive, the PCE of the device improved to 9.28%, which implies that additives are a powerful tool to regulate the device performance. Yan *et al.* reported three PDI-based molecules **10**, **11**, and **12** with different fusions to the core benzene ring. The three materials were employed as acceptors to build OSC devices, and compared with the blend film of precursor of **12**, the blend film of **12** presented an enhanced degree of ordering and larger coherence length, which was beneficial for the device FF and J_{sc}, generating a higher PCE (Fig. 15c). It is suggested that ring-fused PDI-based materials perform better than non-fused materials in OSC devices.

The properties of the molecules mentioned herein that are qualified for use in OSCs are summarized in Fig. 16. Although these properties lag behind current developments, they provide an impressive and sharp understanding of the structure–property-performance relationship in OSCs.

3.3. Other applications

Superconductivity. Superconductivity is a unique physical phenomenon, which has attracted great interest. As early as 1964, the American scientist Little boldly proposed a model that suggests organic molecules also have the possibility of superconductivity.[144] This greatly encouraged further research. With the development of their understanding, scientists are conscious that an ideal organic superconducting chain requires π electrons to travel in molecules with exactly the same length of single and double bonds for superconductivity.[145] Accordingly, the benzene ring is a hexagon satisfying these conditions and molecules based on the benzene ring skeleton can achieve superconductivity. In 2010, Kubozono and co-workers discovered that **23** intercalated by an alkali metal, forming a black power, produced superconductivity (Fig. 17a).[146] The superconducting

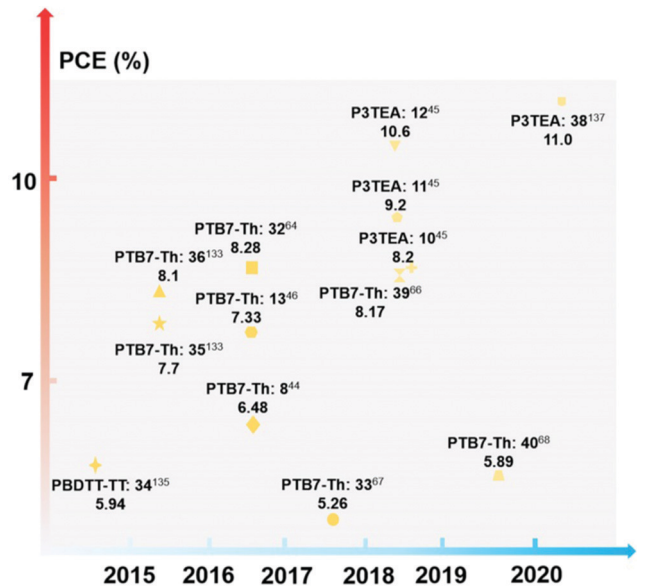

Fig. 16 Summary of the power conversion efficiency (PCE) based on the acceptor in this part. (PTB7-Th: poly[4,8-bis(5-(2-ethylhexyl)thiophen-2-yl)benzo[1,2-*b*;4,5-*b*′]dithiophene-2,6-diyl-*alt*-(4-(2-ethylhexyl)-3-fluorothieno[3,4-*b*]thiophene-)-2-carboxylate-2-6-diyl)]; PBDTT-TT: poly[4,8-bis(5(2-ethylhexyl)thiophen-2-yl)benzo[1,2-*b*;4,5-*b*′]dithiophene2,6-diyl-*alt*-(4-(2-ethylhexyl)-3-fluorothieno[3,4-*b*]thiophene)2-carboxy late-2,6-diyl]; and P3TEA:poly[2-octyldodecyl 5-(5,6-difluoro-7-(4′-(2-hexylnonyl)-5′-methyl-3-(((2-octyldodecyl)oxy)carbonyl)-[2,2′-bithiophen]-5-yl)benzo[c][1,2,5]thiadia zol-4-yl)-5″-(5,6-difluoro-7-(5-methylthiophen-2-yl)benzo[c][1,2,5]thiadiazol-4-yl)-4′-(2-hexylnonyl)-[2,2′:5′,2″-terthiophene]-3-carboxylate].).

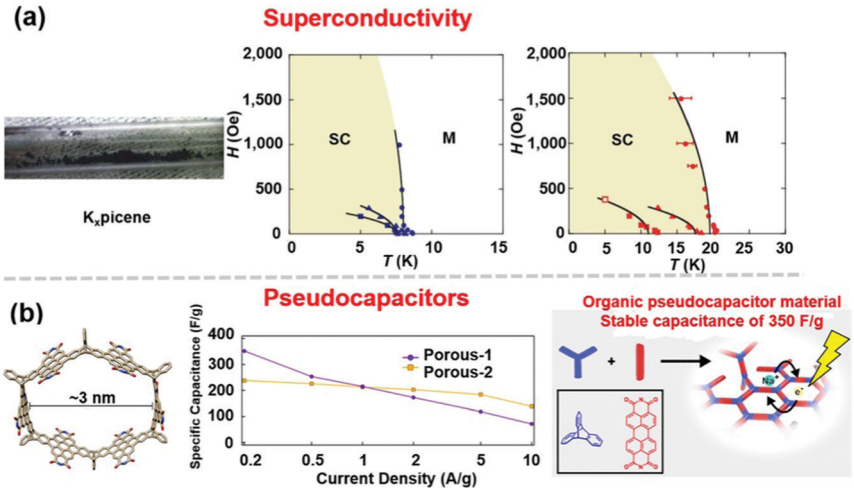

Fig. 17 Applications in superconductivity and pseudocapactiors. (a) K$_x$picene and its superconducting phase diagrams. Reprinted with permission from ref. 146. Copyright 2010, Macmillan Publishers Limited. (b) Molecule structure of porous-2 and its performance in pseudocapactiors. Reprinted with permission from ref. 147. Copyright 2018, the American Chemical Society.

transition temperature of this binary system was found to be 7 K and 18 K, depending on the metal content.

Pseudocapacitors. Pseudocapacitors are energy storage devices that store energy from electrochemical processes. This type of device inherits the elements from both batteries and capacitors and it is expected to be widely used in areas such as new energy vehicles. Nuckolls *et al.* designed a new porous structure based on triptycene subunits and PDI.[147] The architecture after photocyclization contained multiple pores with a diameter size of approximately 3 nm and possessed a high internal surface area (Fig. 17b). The pseudocapacitor constructed using porous-2 displayed capacitance values of up to 190 F g^{-1} and little decay in capacitance after 10 000 cycles. Although the capacitance of porous-2 was lower than that of porous-1 (350 F g^{-1}), the variation from porous-1 to porous-2 demonstrated the tunability of the material performance.

4. Conclusions

PAH-based materials are endowed with attractive optical, electrical, magnetic and even chiral features due to their large π-conjugated planes and unique structures. These abundant molecular species and properties further stimulate their potential applications in various organic optoelectronic devices. In this review, initially, we presented the typical ring-closing reactions, including the Scholl-type reactions, iodine-promoted photocyclization reactions and palladium-catalyzed annulation reactions, and attempted to deliver a summary of the characteristics of these reactions and their application in the synthesis of PAH-based organic semiconductors. Subsequently, the device applications triggered by these PAH materials were also demonstrated with special focus on OFETs, OSCs, and their functional devices, such as chiral OFETs and biradicaloid-based OFETs.

Based on the above review on the development of the PAH field, some perspectives are given as follows: (1) it is essential to further develop and optimize the current ring-closing reactions for precisely synthesizing high-quality and more complex PAHs, which is the premise and basis for achieving much higher performances and exploring novel properties. (2) The internal correlation mechanism between molecular structure and properties should be well established. This is important for appropriately guiding the flowing synthesis of PAHs with oriented function.[148] (3) Efforts should be devoted to developing various PAH materials with novelty and versatility. The most striking feature of PAH materials is their large conjugated system and unique molecular characteristics, which give them the potential to produce interesting optical, electrical and magnetic properties or to break through the current single performance, such as the integration of high mobility and luminescence, which is crucial for next-generation display technology and electrical-pumped lasers.[149–151] Finally, we believe that as more and more efficient synthetic methods are developed, more PAHs with diverse structures and excellent performances, even artistic, will be achieved, which will present uniqueness in the application of functional devices and research on novel physical properties.

Conflicts of interest

The authors declare no conflict of interest.

Acknowledgements

The authors acknowledge financial support from Ministry of Science and Technology of China (2018YFA0703200), National Natural Science Foundation of China (21875259, 61890943, 22021002, 91833306), Beijing National Laboratory for Molecular Sciences (BNLMS-CXXM-202012), the Key Research Program of the Chinese Academy of Sciences (Grant No. XDPB13), the International Cooperation Program of Chinese Academy of Sciences (CJTD-202002, 121111KYSB20200004).

Notes and references

1 H. Jiang and W. Hu, *Angew. Chem., Int. Ed.*, 2020, **59**, 1408–1428.
2 J. Ouyang, *SmartMat*, 2021, **2**, 263–285.
3 H. Dong, X. Fu, J. Liu, Z. Wang and W. Hu, *Adv. Mater.*, 2013, **25**, 6158–6183.
4 G. Hong, X. Gan, C. Leonhardt, Z. Zhang, J. Seibert, J. M. Busch and S. Brase, *Adv. Mater.*, 2021, **33**, e2005630.
5 Z. G. Zhang and Y. Li, *Angew. Chem., Int. Ed.*, 2021, **60**, 4422–4433.
6 C. Wang, H. Dong, W. Hu, Y. Liu and D. Zhu, *Chem. Rev.*, 2012, **112**, 2208–2267.
7 C. Wang, J. Zhang, G. Long, N. Aratani, H. Yamada, Y. Zhao and Q. Zhang, *Angew. Chem., Int. Ed.*, 2015, **54**, 6292–6296.
8 Z. Zhang and Q. Zhang, *Mate. Chem. Front.*, 2020, **4**, 3419–3432.
9 T. W. Kelley, D. V. Muyres, P. F. Baude, T. P. Smith and T. D. Jones, *Mater. Res. Soc. Symp. Proc.*, 2003, **771**, 169.
10 K. Xiao, Y. Liu, T. Qi, W. Zhang, F. Wang, J. Gao, W. Qiu, Y. Ma, G. Cui, S. Chen, X. Zhan, G. Yu, J. Qin, W. Hu and D. Zhu, *J. Am. Chem. Soc.*, 2005, **127**, 13281–13286.
11 R. Scholl and J. Mansfeld, *Ber. Dtsch. Chem. Ges.*, 1910, **43**, 1734–1746.
12 M. Grzybowski, K. Skonieczny, H. Butenschön and D. T. Gryko, *Angew. Chem., Int. Ed.*, 2013, **52**, 9900–9930.
13 W. Chen, F. Yu, Q. Xu, G. Zhou and Q. Zhang, *Adv. Sci.*, 2020, **7**, 1903766.
14 K. B. Jorgensen, *Molecules*, 2010, **15**, 4334–4358.
15 M. Grzybowski, B. Sadowski, H. Butenschon and D. T. Gryko, *Angew. Chem., Int. Ed.*, 2020, **59**, 2998–3027.
16 T. Jin, J. Zhao, N. Asao and Y. Yamamoto, *Chemistry*, 2014, **20**, 3554–3576.
17 A. A. Sarhan and C. Bolm, *Chem. Soc. Rev.*, 2009, **38**, 2730–2744.
18 G. Baddeley and J. Kenner, *J. Chem. Soc.*, 1935, 303–309.
19 W. S. Wong, W. W. Lau, Y. Li, Z. Liu, D. Kuck and H. F. Chow, *Chemistry*, 2020, **26**, 4310–4319.
20 T. Fujikawa, Y. Segawa and K. Itami, *J. Am. Chem. Soc.*, 2016, **138**, 3587–3595.
21 A. Pradhan, P. Dechambenoit, H. Bock and F. Durola, *J. Org. Chem.*, 2013, **78**, 2266–2274.
22 J. Liu, A. Narita, S. Osella, W. Zhang, D. Schollmeyer, D. Beljonne, X. Feng and K. Mullen, *J. Am. Chem. Soc.*, 2016, **138**, 2602–2608.
23 J. M. Fernandez-Garcia, P. J. Evans, S. Medina Rivero, I. Fernandez, D. Garcia-Fresnadillo, J. Perles, J. Casado and N. Martin, *J. Am. Chem. Soc.*, 2018, **140**, 17188–17196.
24 F. B. Mallory, C. S. Wood, J. T. Gordon, L. C. Lindquist and M. L. Savitz, *J. Am. Chem. Soc.*, 1962, **84**, 4361–4362.
25 S. Protti, G. A. Artioli, F. Capitani, C. Marini, P. Dore, P. Postorino, L. Malavasi and M. Fagnoni, *RSC Adv.*, 2015, **5**, 27470–27475.
26 O. Allemann, S. Duttwyler, P. Romanato, K. K. Baldridge and J. S. Siegel, *Science*, 2011, **332**, 574–577.
27 E. A. Jackson, B. D. Steinberg, M. Bancu, A. Wakamiya and L. T. Scott, *J. Am. Chem. Soc.*, 2007, **129**, 484–485.
28 K. Kato, Y. Segawa, L. T. Scott and K. Itami, *Angew. Chem., Int. Ed.*, 2018, **57**, 1337–1341.
29 M. Mahl, K. Shoyama, J. Ruhe, V. Grande and F. Wurthner, *Chemistry*, 2018, **24**, 9409–9416.
30 K. Shoyama, M. Mahl, S. Seifert and F. Wurthner, *J. Org. Chem.*, 2018, **83**, 5339–5346.
31 S. Seifert, D. Schmidt and F. Würthner, *Org. Chem. Front.*, 2016, **3**, 1435–1442.
32 H. Ito, K. Ozaki and K. Itami, *Angew. Chem., Int. Ed.*, 2017, **56**, 11144–11164.
33 K. Ozaki, K. Kawasumi, M. Shibata, H. Ito and K. Itami, *Nat. Commun.*, 2015, **6**, 6251.
34 D. Uersfeld, S. Stappert, C. Li and K. Müllen, *Adv. Synth. Catal.*, 2017, **359**, 4184–4189.
35 W. Yue, A. Lv, J. Gao, W. Jiang, L. Hao, C. Li, Y. Li, L. E. Polander, S. Barlow, W. Hu, S. Di Motta, F. Negri, S. R. Marder and Z. Wang, *J. Am. Chem. Soc.*, 2012, **134**, 5770–5773.
36 W. Yue, J. Gao, Y. Li, W. Jiang, S. Di Motta, F. Negri and Z. Wang, *J. Am. Chem. Soc.*, 2011, **133**, 18054–18057.
37 X. Cui, C. Xiao, T. Winands, T. Koch, Y. Li, L. Zhang, N. L. Doltsinis and Z. Wang, *J. Am. Chem. Soc.*, 2018, **140**, 12175–12180.
38 L. Chen, Y. Hernandez, X. Feng and K. Mullen, *Angew. Chem., Int. Ed.*, 2012, **51**, 7640–7654.
39 X. Xu, K. Müllen and A. Narita, *Bull. Chem. Soc. Jpn.*, 2020, **93**, 490–506.
40 A. Homer, *J. Chem. Soc., Trans.*, 1910, **97**, 1141–1154.
41 M. R. Ajayakumar, Y. Fu, J. Ma, F. Hennersdorf, H. Komber, J. J. Weigand, A. Alfonsov, A. A. Popov, R. Berger, J. Liu, K. Mullen and X. Feng, *J. Am. Chem. Soc.*, 2018, **140**, 6240–6244.
42 J. J. Shen, Y. Han, S. Dong, H. Phan, T. S. Herng, T. Xu, J. Ding and C. Chi, *Angew. Chem., Int. Ed.*, 2021, **60**, 4464–4469.
43 J. Luo, X. Xu, R. Mao and Q. Miao, *J. Am. Chem. Soc.*, 2012, **134**, 13796–13803.
44 H. Zhong, C. H. Wu, C. Z. Li, J. Carpenter, C. C. Chueh, J. Y. Chen, H. Ade and A. K. Jen, *Adv. Mater.*, 2016, **28**, 951–958.
45 H. Hu, Y. Li, J. Zhang, Z. Peng, L. K. Ma, J. Xin, J. Huang, T. Ma, K. Jiang, G. Zhang, W. Ma, H. Ade and H. Yan, *Adv. Energy Mater.*, 2018, **8**, 1800234.
46 S. Li, W. Liu, C.-Z. Li, T.-K. Lau, X. Lu, M. Shi and H. Chen, *J. Mater. Chem. A*, 2016, **4**, 14983–14987.
47 S. Zhang, Y. Guo, Y. Zhang, R. Liu, Q. Li, X. Zhan, Y. Liu and W. Hu, *Chem. Commun.*, 2010, **46**, 2841–2843.
48 X. Liu, Y. Wang, J. Gao, L. Jiang, X. Qi, W. Hao, S. Zou, H. Zhang, H. Li and W. Hu, *Chem. Commun.*, 2014, **50**, 442–444.
49 Y. Wang, S. Zou, J. Gao, H. Zhang, G. Lai, C. Yang, H. Xie, R. Fang, H. Li and W. Hu, *Chem. Commun.*, 2015, **51**, 11961–11963.
50 Z. Sun, S. Lee, K. H. Park, X. Zhu, W. Zhang, B. Zheng, P. Hu, Z. Zeng, S. Das, Y. Li, C. Chi, R. W. Li, K. W. Huang, J. Ding, D. Kim and J. Wu, *J. Am. Chem. Soc.*, 2013, **135**, 18229–18236.

51 H. Yokoi, Y. Hiraoka, S. Hiroto, D. Sakamaki, S. Seki and H. Shinokubo, *Nat. Commun.*, 2015, **6**, 8251.
52 J. Z. Liu, J. Ma, K. Zhang, P. Ravat, P. Machata, S. Avdoshenko, F. Hennersdorf, H. Komber, W. Pisula, J. J. Weigand, A. A. Popov, R. Berger, K. Mullen and X. L. Feng, *J. Am. Chem. Soc.*, 2017, **139**, 7513–7521.
53 S. Seifert, K. Shoyama, D. Schmidt and F. Würthner, *Angew. Chem., Int. Ed.*, 2016, **55**, 6390–6395.
54 G. Gao, M. Chen, J. Roberts, M. Feng, C. Xiao, G. Zhang, S. Parkin, C. Risko and L. Zhang, *J. Am. Chem. Soc.*, 2020, **142**, 2460–2470.
55 H.-Y. Chen, J. Golder, S.-C. Yeh, C.-W. Lin, C.-T. Chen and C.-T. Chen, *RSC Adv.*, 2015, **5**, 3381–3385.
56 F. Aloui, R. E. Abed and B. B. Hassine, *Tetrahedron Lett.*, 2008, **49**, 1455–1457.
57 S. Xiao, J. Tang, T. Beetz, X. Guo, N. Tremblay, T. Siegrist, Y. Zhu, M. Steigerwald and C. Nuckolls, *J. Am. Chem. Soc.*, 2006, **128**, 10700–10701.
58 A. A. Gorodetsky, C. Y. Chiu, T. Schiros, M. Palma, M. Cox, Z. Jia, W. Sattler, I. Kymissis, M. Steigerwald and C. Nuckolls, *Angew. Chem., Int. Ed.*, 2010, **49**, 7909–7912.
59 S. Xiao, S. J. Kang, Y. Zhong, S. Zhang, A. M. Scott, A. Moscatelli, N. J. Turro, M. L. Steigerwald, H. Li and C. Nuckolls, *Angew. Chem., Int. Ed.*, 2013, **52**, 4558–4562.
60 H. Usta, C. Newman, Z. Chen and A. Facchetti, *Adv. Mater.*, 2012, **24**, 3678–3684.
61 N. Liang, D. Meng and Z. Wang, *Acc. Chem. Res.*, 2021, **54**, 961–975.
62 D. Meng, G. Liu, C. Xiao, Y. Shi, L. Zhang, L. Jiang, K. K. Baldridge, Y. Li, J. S. Siegel and Z. Wang, *J. Am. Chem. Soc.*, 2019, **141**, 5402–5408.
63 Y. Zhong, B. Kumar, S. Oh, M. T. Trinh, Y. Wu, K. Elbert, P. Li, X. Zhu, S. Xiao, F. Ng, M. L. Steigerwald and C. Nuckolls, *J. Am. Chem. Soc.*, 2014, **136**, 8122–8130.
64 D. Meng, H. Fu, C. Xiao, X. Meng, T. Winands, W. Ma, W. Wei, B. Fan, L. Huo, N. L. Doltsinis, Y. Li, Y. Sun and Z. Wang, *J. Am. Chem. Soc.*, 2016, **138**, 10184–10190.
65 B. Liu, M. Bockmann, W. Jiang, N. L. Doltsinis and Z. Wang, *J. Am. Chem. Soc.*, 2020, **142**, 7092–7099.
66 M. Wu, J. P. Yi, L. Chen, G. He, F. Chen, M. Y. Sfeir and J. Xia, *ACS Appl. Mater. Interfaces*, 2018, **10**, 27894–27901.
67 D. Meng, H. Fu, B. Fan, J. Zhang, Y. Li, Y. Sun and Z. Wang, *Chem. – Asian J.*, 2017, **12**, 1286–1290.
68 Y. Yin, Z. Zheng, D. Chen, M. Liu, J. Zhang, F. Guo, S. Gao, L. Zhao and Y. Zhang, *J. Mater. Chem. A*, 2019, **7**, 27493–27502.
69 P. E. Hartnett, H. Matte, N. D. Eastham, N. E. Jackson, Y. Wu, L. X. Chen, M. A. Ratner, R. P. H. Chang, M. C. Hersam, M. R. Wasielewski and T. J. Marks, *Chem. Sci.*, 2016, **7**, 3543–3555.
70 G. Liu, T. Koch, Y. Li, N. L. Doltsinis and Z. Wang, *Angew. Chem., Int. Ed.*, 2019, **58**, 178–183.
71 R. Huang, H. Phan, T. S. Herng, P. Hu, W. Zeng, S. Q. Dong, S. Das, Y. Shen, J. Ding, D. Casanova and J. Wu, *J. Am. Chem. Soc.*, 2016, **138**, 10323–10330.
72 W. Zeng, T. Y. Gopalakrishna, H. Phan, T. Tanaka, T. S. Herng, J. Ding, A. Osuka and J. Wu, *J. Am. Chem. Soc.*, 2018, **140**, 14054–14058.
73 W. Zeng, Z. Sun, T. S. Herng, T. P. Goncalves, T. Y. Gopalakrishna, K. W. Huang, J. Ding and J. Wu, *Angew. Chem., Int. Ed.*, 2016, **55**, 8615–8619.
74 C. Zong, X. Zhu, Z. Xu, L. Zhang, J. Xu, J. Guo, Q. Xiang, Z. Zeng, W. Hu, J. Wu, R. Li and Z. Sun, *Angew. Chem., Int. Ed.*, 2021, **60**, 16230–16236.
75 L. Zhang, A. Fonari, Y. Liu, A. L. Hoyt, H. Lee, D. Granger, S. Parkin, T. P. Russell, J. E. Anthony, J. L. Bredas, V. Coropceanu and A. L. Briseno, *J. Am. Chem. Soc.*, 2014, **136**, 9248–9251.
76 T. Jousselin-Oba, M. Mamada, J. Marrot, A. Maignan, C. Adachi, A. Yassar and M. Frigoli, *J. Am. Chem. Soc.*, 2019, **141**, 9373–9381.
77 G. E. Rudebusch, J. L. Zafra, K. Jorner, K. Fukuda, J. L. Marshall, I. Arrechea-Marcos, G. L. Espejo, R. Ponce Ortiz, C. J. Gomez-Garcia, L. N. Zakharov, M. Nakano, H. Ottosson, J. Casado and M. M. Haley, *Nat. Chem.*, 2016, **8**, 753–759.
78 T. Jousselin-Oba, M. Mamada, A. Okazawa, J. Marrot, T. Ishida, C. Adachi, A. Yassar and M. Frigoli, *Chem. Sci.*, 2020, **11**, 12194–12205.
79 Y.-C. Hsieh, C.-F. Wu, Y.-T. Chen, C.-T. Fang, C.-S. Wang, C.-H. Li, L.-Y. Chen, M.-J. Cheng, C.-C. Chueh, P.-T. Chou and Y.-T. Wu, *J. Am. Chem. Soc.*, 2018, **140**, 14357–14366.
80 G. Zhang, F. Rominger, U. Zschieschang, H. Klauk and M. Mastalerz, *Chemistry*, 2016, **22**, 14840–14845.
81 J. Liu, S. Mishra, C. A. Pignedoli, D. Passerone, J. I. Urgel, A. Fabrizio, T. G. Lohr, J. Ma, H. Komber, M. Baumgarten, C. Corminboeuf, R. Berger, P. Ruffieux, K. Mullen, R. Fasel and X. Feng, *J. Am. Chem. Soc.*, 2019, **141**, 12011–12020.
82 J. Ma, J. Liu, M. Baumgarten, Y. Fu, Y.-Z. Tan, K. S. Schellhammer, F. Ortmann, G. Cuniberti, H. Komber, R. Berger, K. Müllen and X. Feng, *Angew. Chem., Int. Ed.*, 2017, **56**, 3280–3284.
83 X. Zhang, X. Jiang, K. Zhang, L. Mao, J. Luo, C. Chi, H. S. Chan and J. Wu, *J. Org. Chem.*, 2010, **75**, 8069–8077.
84 A. Konishi, Y. Hirao, M. Nakano, A. Shimizu, E. Botek, B. Champagne, D. Shiomi, K. Sato, T. Takui, K. Matsumoto, H. Kurata and T. Kubo, *J. Am. Chem. Soc.*, 2010, **132**, 11021–11023.
85 A. Konishi, Y. Hirao, K. Matsumoto, H. Kurata, R. Kishi, Y. Shigeta, M. Nakano, K. Tokunaga, K. Kamada and T. Kubo, *J. Am. Chem. Soc.*, 2013, **135**, 1430–1437.
86 M. R. Ajayakumar, J. Ma, A. Lucotti, K. S. Schellhammer, G. Serra, E. Dmitrieva, M. Rosenkranz, H. Komber, J. Liu, F. Ortmann, M. Tommasini and X. Feng, *Angew. Chem., Int. Ed.*, 2021, **60**, 13853–13858.
87 Q. Shi, X. Shi, C. Feng, Y. Wu, N. Zheng, J. Liu, X. Wu, H. Chen, A. Peng, J. Li, L. Jiang, H. Fu, Z. Xie, S. R. Marder, S. B. Blakey and H. Huang, *Angew. Chem., Int. Ed.*, 2021, **60**, 2924–2928.
88 Y. S. Park, D. J. Dibble, J. Kim, R. C. Lopez, E. Vargas and A. A. Gorodetsky, *Angew. Chem., Int. Ed.*, 2016, **55**, 3352–3355.

89 Y. Yang, Z. Liu, G. Zhang, X. Zhang and D. Zhang, *Adv. Mater.*, 2019, **31**, e1903104.
90 Z. Wang, P. Gu, G. Liu, H. Yao, Y. Wu, Y. Li, G. Rakesh, J. Zhu, H. Fu and Q. Zhang, *Chem. Commun.*, 2017, **53**, 7772–7775.
91 W. Chen, X. Li, G. Long, Y. Li, R. Ganguly, M. Zhang, N. Aratani, H. Yamada, M. Liu and Q. Zhang, *Angew. Chem., Int. Ed.*, 2018, **57**, 13555–13559.
92 A. M. van de Craats, N. Stutzmann, O. Bunk, M. M. Nielsen, M. Watson, K. Müllen, H. D. Chanzy, H. Sirringhaus and R. H. Friend, *Adv. Mater.*, 2003, **15**, 495–499.
93 J. P. Hill, W. Jin, A. Kosaka, T. Fukushima, H. Ichihara, T. Shimomura, K. Ito, T. Hashizume, N. Ishii and T. Aida, *Science*, 2004, **304**, 1481–1483.
94 Y. Yamamoto, T. Fukushima, Y. Suna, N. Ishii, A. Saeki, S. Seki, S. Tagawa, M. Taniguchi, T. Kawai and T. Aida, *Science*, 2006, **314**, 1761–1764.
95 Y. Zhang, H. Dong, Q. Tang, S. Ferdous, F. Liu, S. C. Mannsfeld, W. Hu and A. L. Briseno, *J. Am. Chem. Soc.*, 2010, **132**, 11580–11584.
96 S. Kumar, S. Pola, C. W. Huang, M. M. Islam, S. Venkateswarlu and Y. T. Tao, *J. Org. Chem.*, 2019, **84**, 8562–8570.
97 S. Pola, C.-H. Kuo, W.-T. Peng, M. M. Islam, I. Chao and Y.-T. Tao, *Chem. Mater.*, 2012, **24**, 2566–2571.
98 X. Fu, Y. Zhen, Z. Ni, Y. Li, H. Dong, J. S. Siegel and W. Hu, *Angew. Chem., Int. Ed.*, 2020, **59**, 14024–14028.
99 B. Fu, X. Hou, C. Wang, Y. Wang, X. Zhang, R. Li, X. Shao and W. Hu, *Chem. Commun.*, 2017, **53**, 11407–11409.
100 L. Tan, W. Jiang, L. Jiang, S. Jiang, Z. Wang, S. Yan and W. Hu, *Appl. Phys. Lett.*, 2009, **94**, 153306.
101 Y. Yin, J. Song, F. Guo, Y. Sun, L. Zhao and Y. Zhang, *ACS Appl. Energy Mater.*, 2018, **1**, 6577–6585.
102 J. Mei, Y. Diao, A. L. Appleton, L. Fang and Z. Bao, *J. Am. Chem. Soc.*, 2013, **135**, 6724–6746.
103 X. Gu, L. Shaw, K. Gu, M. F. Toney and Z. Bao, *Nat. Commun.*, 2018, **9**(1), 534.
104 X. Yu, C. Li, C. Gao, X. Zhang, G. Zhang and D. Zhang, *SmartMat*, 2021, **2**, 347–366.
105 Y. Yao, H. Dong and W. Hu, *Adv. Mater.*, 2016, **28**, 4513–4523.
106 C.-T. Hsieh, C.-Y. Chen, H.-Y. Lin, C.-J. Yang, T.-J. Chen, K.-Y. Wu and C.-L. Wang, *J. Phys. Chem. C*, 2018, **122**, 16242–16248.
107 W. Pisula, A. Menon, M. Stepputat, I. Lieberwirth, U. Kolb, A. Tracz, H. Sirringhaus, T. Pakula and K. Müllen, *Adv. Mater.*, 2005, **17**, 684–689.
108 J. Wu, W. Pisula and K. Mullen, *Chem. Rev.*, 2007, **107**, 718–747.
109 A. M. Hiszpanski, A. R. Woll, B. Kim, C. Nuckolls and Y.-L. Loo, *Chem. Mater.*, 2017, **29**, 4311–4316.
110 X. Guo, S. Xiao, M. Myers, Q. Miao, M. L. Steigerwald and C. Nuckolls, *Proc. Natl. Acad. Sci. U. S. A.*, 2009, **106**, 691–696.
111 X. Guo, M. Myers, S. Xiao, M. Lefenfeld, R. Steiner, G. S. Tulevski, J. Tang, J. Baumert, F. Leibfarth, J. T. Yardley, M. L. Steigerwald, P. Kim and C. Nuckolls, *Proc. Natl. Acad. Sci. U. S. A.*, 2006, **103**, 11452–11456.
112 C.-H. Kuo, D.-C. Huang, W.-T. Peng, K. Goto, I. Chao and Y.-T. Tao, *J. Mater. Chem. C*, 2014, **2**, 3928–3935.
113 Y. Huang, Z. Wang, Z. Chen and Q. Zhang, *Angew. Chem., Int. Ed.*, 2019, **58**, 9696–9711.
114 L. Sun, W. Zhu, X. Zhang, L. Li, H. Dong and W. Hu, *J. Am. Chem. Soc.*, 2021, **143**, 19243–19256.
115 Y. Wang, Y. Li, W. Zhu, J. Liu, X. Zhang, R. Li, Y. Zhen, H. Dong and W. Hu, *Nanoscale*, 2016, **8**, 14920–14924.
116 Y. Sun, Y. Lei, H. Dong, Y. Zhen and W. Hu, *J. Am. Chem. Soc.*, 2018, **140**, 6186–6189.
117 W. Zhu, X. Zhang and W. Hu, *Sci. Bull.*, 2021, **66**, 512–520.
118 M. Gingras, *Chem. Soc. Rev.*, 2013, **42**, 968–1006.
119 Y. Yang, B. Rice, X. Shi, J. R. Brandt, R. Correa da Costa, G. J. Hedley, D. M. Smilgies, J. M. Frost, I. D. W. Samuel, A. Otero-de-la-Roza, E. R. Johnson, K. E. Jelfs, J. Nelson, A. J. Campbell and M. J. Fuchter, *ACS Nano*, 2017, **11**, 8329–8338.
120 C. Shen, G. Zhang, Y. Ding, N. Yang, F. Gan, J. Crassous and H. Qiu, *Nat. Commun.*, 2021, **12**, 2786.
121 Y. Yang, R. C. da Costa, M. J. Fuchter and A. J. Campbell, *Nat. Photonics*, 2013, **7**, 634–638.
122 D. Aranda, N. J. Schuster, X. Xiao, F. J. Ávila Ferrer, F. Santoro and C. Nuckolls, *J. Phys. Chem. C*, 2021, **125**, 2554–2564.
123 L. Zhang, I. Song, J. Ahn, M. Han, M. Linares, M. Surin, H. J. Zhang, J. H. Oh and J. Lin, *Nat. Commun.*, 2021, **12**, 142.
124 M. Nakano, *Chem. Rec.*, 2017, **17**, 27–62.
125 T. Kubo, A. Shimizu, M. Sakamoto, M. Uruichi, K. Yakushi, M. Nakano, D. Shiomi, K. Sato, T. Takui, Y. Morita and K. Nakasuji, *Angew. Chem., Int. Ed.*, 2005, **44**, 6564–6568.
126 A. Shimizu, Y. Hirao, K. Matsumoto, H. Kurata, T. Kubo, M. Uruichi and K. Yakushi, *Chem. Commun.*, 2012, **48**, 5629–5631.
127 A. Shimizu, T. Kubo, M. Uruichi, K. Yakushi, M. Nakano, D. Shiomi, K. Sato, T. Takui, Y. Hirao, K. Matsumoto, H. Kurata, Y. Morita and K. Nakasuji, *J. Am. Chem. Soc.*, 2010, **132**, 14421–14428.
128 M. Mamada, R. Nakamura and C. Adachi, *Chem. Sci.*, 2021, **12**, 552–558.
129 Z. Sun, K. W. Huang and J. Wu, *J. Am. Chem. Soc.*, 2011, **133**, 11896–11899.
130 A. Shimizu, R. Kishi, M. Nakano, D. Shiomi, K. Sato, T. Takui, I. Hisaki, M. Miyata and Y. Tobe, *Angew. Chem., Int. Ed.*, 2013, **52**, 6076–6079.
131 H. Miyoshi, M. Miki, S. Hirano, A. Shimizu, R. Kishi, K. Fukuda, D. Shiomi, K. Sato, T. Takui, I. Hisaki, M. Nakano and Y. Tobe, *J. Org. Chem.*, 2017, **82**, 1380–1388.
132 A. M. Zeidell, L. Jennings, C. K. Frederickson, Q. Ai, J. J. Dressler, L. N. Zakharov, C. Risko, M. M. Haley and O. D. Jurchescu, *Chem. Mater.*, 2019, **31**, 6962–6970.
133 J. J. Dressler, M. Teraoka, G. L. Espejo, R. Kishi, S. Takamuku, C. J. Gomez-Garcia, L. N. Zakharov,

M. Nakano, J. Casado and M. M. Haley, *Nat. Chem.*, 2018, **10**, 1134–1140.
134 Y. Li, G. Xu, C. Cui and Y. Li, *Adv. Energy Mater.*, 2018, **8**, 1701791.
135 Y. Lin, J. Wang, Z. G. Zhang, H. Bai, Y. Li, D. Zhu and X. Zhan, *Adv. Mater.*, 2015, **27**, 1170–1174.
136 J. Yuan, Y. Zhang, L. Zhou, G. Zhang, H.-L. Yip, T.-K. Lau, X. Lu, C. Zhu, H. Peng, P. A. Johnson, M. Leclerc, Y. Cao, J. Ulanski, Y. Li and Y. Zou, *Joule*, 2019, **3**, 1140–1151.
137 S. D. Collins, N. A. Ran, M. C. Heiber and T.-Q. Nguyen, *Adv. Energy Mater.*, 2017, **7**, 1602242.
138 Y. Zhong, M. T. Trinh, R. Chen, G. E. Purdum, P. P. Khlyabich, M. Sezen, S. Oh, H. Zhu, B. Fowler, B. Zhang, W. Wang, C. Y. Nam, M. Y. Sfeir, C. T. Black, M. L. Steigerwald, Y. L. Loo, F. Ng, X. Y. Zhu and C. Nuckolls, *Nat. Commun.*, 2015, **6**, 8242.
139 Y. Li, L. Yu, L. Chen, C. Han, H. Jiang, Z. Liu, N. Zheng, J. Wang, M. Sun, R. Yang and X. Bao, *Innovation*, 2021, **2**, 100090.
140 W. Zhu, A. P. Spencer, S. Mukherjee, J. M. Alzola, V. K. Sangwan, S. H. Amsterdam, S. M. Swick, L. O. Jones, M. C. Heiber, A. A. Herzing, G. Li, C. L. Stern, D. M. DeLongchamp, K. L. Kohlstedt, M. C. Hersam, G. C. Schatz, M. R. Wasielewski, L. X. Chen, A. Facchetti and T. J. Marks, *J. Am. Chem. Soc.*, 2020, **142**, 14532–14547.
141 Y. Zhong, M. T. Trinh, R. Chen, W. Wang, P. P. Khlyabich, B. Kumar, Q. Xu, C. Y. Nam, M. Y. Sfeir, C. Black, M. L. Steigerwald, Y. L. Loo, S. Xiao, F. Ng, X. Y. Zhu and C. Nuckolls, *J. Am. Chem. Soc.*, 2014, **136**, 15215–15221.
142 S. Chen, D. Meng, J. Huang, N. Liang, Y. Li, F. Liu, H. Yan and Z. Wang, *CCS Chem.*, 2021, **3**, 78–84.
143 X. Liu, Y. Cai, X. Huang, R. Zhang and X. Sun, *J. Mater. Chem. C*, 2017, **5**, 3188–3194.
144 W. A. Little, *Phys. Rev.*, 1964, **134**, A1416.
145 M. Xue, T. Cao, D. Wang, Y. Wu, H. Yang, X. Dong, J. He, F. Li and G. F. Chen, *Sci. Rep.*, 2012, **2**, 389.
146 R. Mitsuhashi, Y. Suzuki, Y. Yamanari, H. Mitamura, T. Kambe, N. Ikeda, H. Okamoto, A. Fujiwara, M. Yamaji, N. Kawasaki, Y. Maniwa and Y. Kubozono, *Nature*, 2010, **464**, 76–79.
147 S. R. Peurifoy, J. C. Russell, T. J. Sisto, Y. Yang, X. Roy and C. Nuckolls, *J. Am. Chem. Soc.*, 2018, **140**, 10960–10964.
148 H. Ju, K. Wang, J. Zhang, H. Geng, Z. Liu, G. Zhang, Y. Zhao and D. Zhang, *Chem. Mater.*, 2017, **29**, 3580–3588.
149 J. Liu, H. Zhang, H. Dong, L. Meng, L. Jiang, L. Jiang, Y. Wang, J. Yu, Y. Sun, W. Hu and A. J. Heeger, *Nat. Commun.*, 2015, **6**, 10032.
150 Z. Qin, H. Gao, H. Dong and W. Hu, *Adv. Mater.*, 2021, **33**, e2007149.
151 C. Gao, W. W. H. Wong, Z. Qin, S. C. Lo, E. B. Namdas, H. Dong and W. Hu, *Adv. Mater.*, 2021, **33**, e2100704.

